HOT SPOT DISSIPATION IN 3D STACKS

Electronics COOLING

JUNE 2012

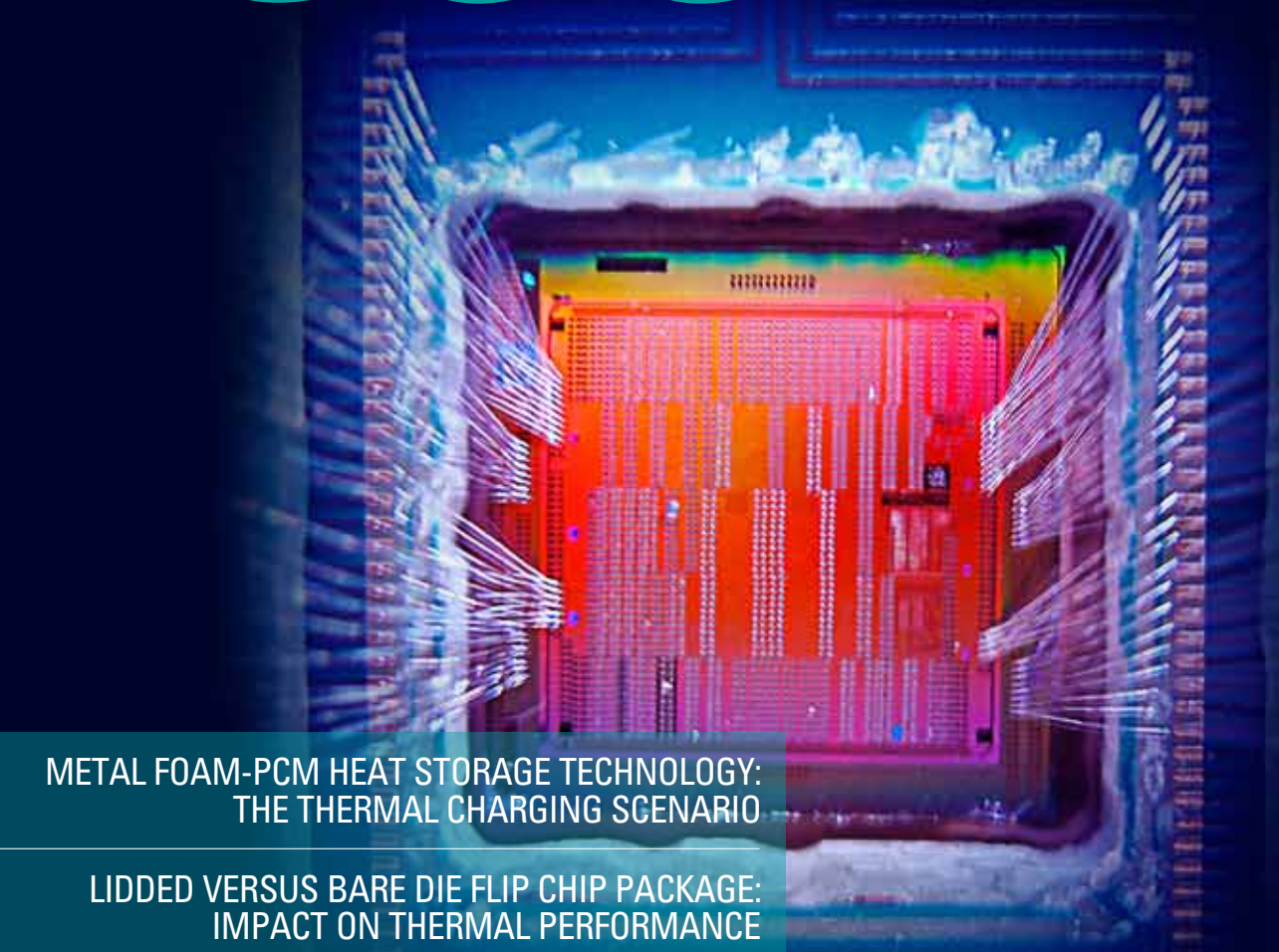

METAL FOAM-PCM HEAT STORAGE TECHNOLOGY: THE THERMAL CHARGING SCENARIO

LIDDED VERSUS BARE DIE FLIP CHIP PACKAGE: IMPACT ON THERMAL PERFORMANCE

electronics-cooling.com

SPRAY COOLING

Thermal Challenge: VRM

High Ambient / High Watt Dissipation / Low Air Flow

Solution: New Bergquist S-Class Gap Pad® 5000S35

Gap Pad 5000S35's natural tack makes application clean and easy to handle.

Gap Pad S-Class is perfectly suited for high performance applications such as VRMs, BGAs and ASICs.

Bergquist's newest S-Class is the perfect combination of softness, low thermal resistance and high thermal conductivity. With a low bulk hardness (35 Shore 00) and high thermal conductivity (5.0 W/m-K) it conforms to demanding contours while maintaining its structural integrity. It is an ideal gap filling solution for applications with fragile components that can be damaged by harder materials that cause higher mounting pressure on components. Gap Pad 5000S35 is also an excellent solution for DVD drives, memory modules, and PC boards to chassis.

Excellent interfacing and wet-out makes GP 5000S35 ideal for fragile components with demanding contours and stack-up tolerances.

Ultra soft S-Class integrity offers easy application.

Gap Pad 5000S35 has a natural tack that eliminates the need for additional adhesive layers that can inhibit thermal performance. Its super soft, yet elastic nature provides excellent interfacing and wet-out, even to surfaces with high roughness or topography. Gap Pad 5000S35 features an embedded-fiberglass reinforcement that makes it puncture, shear and tear resistant. No tearing, flaking or crumbling – just clean and easy handling during the assembly process.

FREE S-Class swatch kit.

Visit our web site or call to qualify for your FREE S-Class swatch kit with product details.

FREE Gap Pad S-Class Swatch Kit

Call **1.800.347.4572** or visit **www.bergquistcompany.com/coolrun**

THE BERGQUIST COMPANY

18930 West 78th Street • Chanhassen, MN 55317 • A ISO9001:2000 registered facility
(800) 347-4572 • Phone (952) 835-2322 • Fax (952) 835-0430 • www.bergquistcompany.com

Thermal Materials • Thermal Substrates • Fans and Blowers

Contents

Electronics Cooling | June 2012

Feature Articles

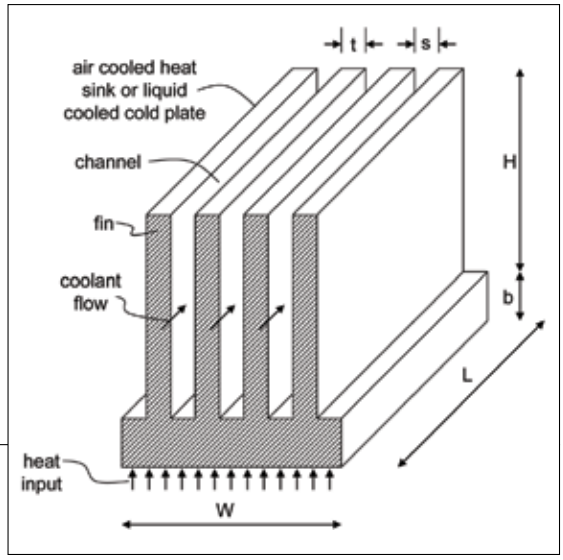

Editorial

My Personal Thermal Management Project

Bruce Guenin, Editor-in-Chief, June 2012

IT CAN BE AN AMUSING THING TO NOTICE HOW sometimes things come full-circle in our lives. My involvement with heat transfer began in college and continued through grad school and a post doc, as I conducted experiments involving liquid helium, both as a refrigerant and the object of study. Since liquid helium was such a precious refrigerant, a key strategy for achieving these temperatures was to minimize the flow of heat into the coldest part of the apparatus.

Fast forward twenty years to 2001. By that time I had been involved in electronics cooling for ten years, and my wife and I were relocating to San Diego. My previous companies in this field were in Connecticut and Arizona. We were moving to the land of near perfect weather, ocean breezes and palm trees. We knew that we would never again have to live among the weather extremes of heat and cold that we had in our previous locales.

As I was settling into my new job, we began looking for a home in our new location. This was a painful process that took 6 months, due to the well-publicized challenges in the California housing market.

Imagine our delight when, due to my wife's detective work, we found a house that was a well maintained, mid-century-modern design, with vaulted ceilings, large exposed wood beams, and a wall of glass providing a panoramic view of Mission Bay from its perch on Mt. Soledad. The doors were all wide open and, thanks to the mild spring day and an ocean breeze, it was very comfortable inside the house, without the assistance of air conditioning— which was a good thing because it had none.

As we were moving into the house in July, we came to the startling realization that our dream home became an oven in the summer months. My inner thermal engineer instantly realized that those very features that attracted us to the house made it very unpleasant during those months with long days of intense sunshine, despite the quite comfortable outside air temperatures. The vaulted ceiling was made possible by not having an attic over most of the house. Hence, a mere 5 cm of wooden boards and asphalt shingles was all that stood between us and the summer sunshine. The wall of single-pane glass allowed the sunlight to pass nearly undiminished into the main living area.

My first impulse was to do what any data center manager would do— throw more fans at the problem. In time, I located three advanced whole house fan units and installed them. All were mounted near the roofline to exhaust the hottest air in the house.

The level of success that I had was comparable to that of our imaginary data center manager— it cooled the house down, but at a cost of a 2x increase in our electrical bill and near deafening noise from the most powerful fan when it was running at high speed.

At this point, my inner cryogenic physicist entered the conversation and suggested that the source of my problem was thermal radiation that was heating our living space. If I dealt with that well enough, then the fans would not have to work as hard.

Since then, we have installed a new roof over our old one with a thick layer of rigid foam insulation between them and retractable sun screens on all the windows. Our house is now comfortable without air conditioning, except on the very hottest days. The fans have been demoted to a supporting (and quieter) role.

The end result is satisfying both personally and professionally. We've achieved an acceptable level of comfort in a manner that is economical and environmentally friendly. I even hear that data center managers are beginning to think in those terms as well.

Following up on Jim Wilson's editorial in the last issue. I'd like to acknowledge all of Bob Simon's contributions to this publication. It was a particular pleasure for me to collaborate with him on the Calculation Corner column. I'm happy to welcome Bob's successor, Madhu Iyengar, who has published his first Calculation Corner in this issue.

Electronics COOLING

www.electronics-cooling.com

PUBLISHED BY
ITEM Media
1000 Germantown Pike, F-2
Plymouth Meeting, PA 19462 USA
Phone: +1 484-688-0300
Fax: +1 484-688-0303
info@electronics-cooling.com
www.electronics-cooling.com

PRESIDENT
Graham Kilshaw
gkilshaw@item-media.net

PUBLISHER
Paul Salotto
psalotto@electronics-cooling.com

ASSISTANT EDITOR
Cait O'Driscoll
codriscoll@item-media.com

GRAPHIC DESIGNER
Evan Schmidt
eschmidt@item-media.net

REPRINTS
Reprints are available on a custom basis at reasonable prices in quantities of 500 or more. Please call +1 484-688-0300.

SUBSCRIPTIONS
Subscription for this quarterly publication is FREE. Subscribe online at:
www.electronics-cooling.com

ITEM MEDIA

Produced by ITEM Media

SUNON

Rely on SUNON

Thermal Solutions just got easy.

Ultra-light, slim, mini compact size.

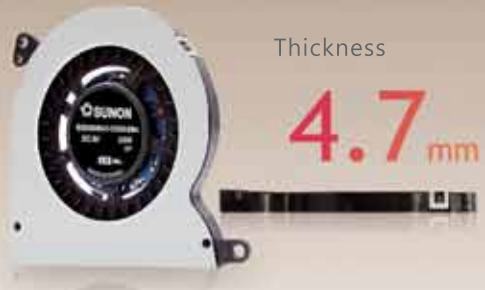

Revolutionary

Ultra slim 4.7mm

Lighter weight 13g

Power saving 24%

Sunonwealth Electric Machine Industry Co., Ltd

Headquarters (Taiwan) URL : www.sunon.com

Sunon Inc. (U.S.A.) URL : www.sunonamerica.com | E-mail : info@sunon.com | Phone : +1-714-255-0208

Time Dependent

Responses and Superposition

Jim Wilson, Associate Technical Editor

ONE OF THE "fairy tales" that I see as a trend in thermal engineers performing electronics cooling is that they become dependent on the capabilities and methodology of the particular software they use. If the help guide or our mentor showed us how to solve a particular problem with our software tool and it worked, we may not have a reason to change even if the method is not the most efficient one. Frequently, we learned some math in school, but do not take advantage of all the tools and techniques our teachers required and encouraged us to master. The topic for this column is superposition with transient information and the fact is that the application of superposition can be very beneficial in assessing time dependent information. As a general topic, superposition has been mentioned in Electronics Cooling a few times [1], but not specifically in this manner.

It is helpful to remind readers that the principle of superposition is applicable only for linear systems. In the electronics cooling field, this usually means that the thermal properties may be assumed constant, radiation effects are minimal, and convection may be represented in a linear fashion (such as a constant heat transfer coefficient back to a constant reference temperature). While there are always exceptions, many of the problems we solve are reasonably well represented by a linear model.

Assessing the dynamic thermal response of electronics systems is a reasonable expectation from a thermal design engineer. Two of the most common questions regarding the transient thermal response of electronics system that I have been asked are:

1. How long does it take to heat up and, related, how long to cool down?
2. What happens if the electronics are turned on and off?

The use of superposition in the time domain is a very useful tool to answer these types of questions and is briefly illustrated by the following example.

Consider a simple thermal system illustrated in Figure 1. The system consists of a few different materials and interfaces and a constant convective boundary condition on the lower surface to a constant reference temperature with all of the other surfaces assumed adiabatic. For the purposes of this column, a numerical model was created with the thermal properties and heat load adjusted such that the temperature response to a step change in the heat value and measured at the center of the heated area results in the time-temperature curve shown in Figure 2a and 2b. The initial temperature was set to a uniform value and both the initial temperature and the reference temperature were set to zero to simplify the use of superposition. Note that the system has an initial rate of temperature increase (in the first unit of time) that is rapid compared to the rate of temperature increase at later times. By about 15 time units, the system has achieved steady-state.

Figure 2a and 2b both contain the same information, but plotted on both a linear and logarithmic time scale. The advantage of plotting the response on a log scale for time (2b) is that the different materials and interfaces may be seen. Assuming that the response is accurate in time and space, this

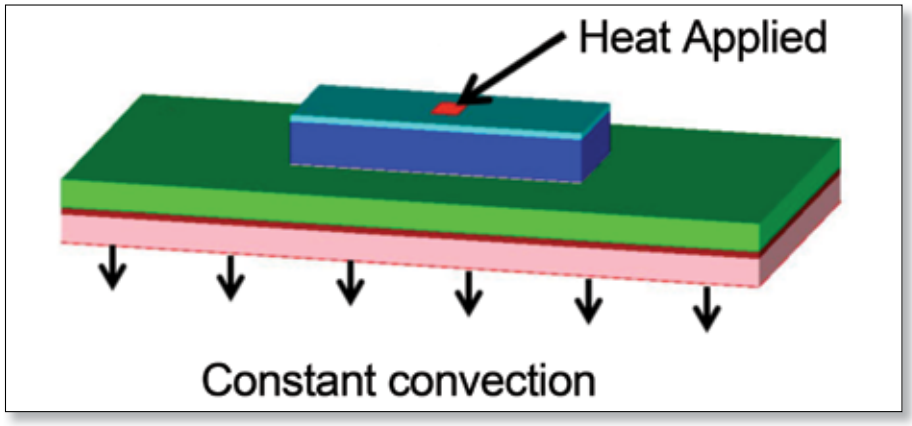

FIGURE 1: Simple electronics system.

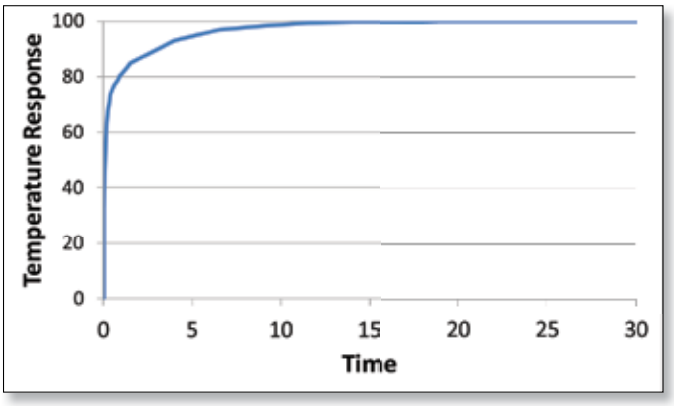

FIGURE 2a: Transient response (linear time scale).

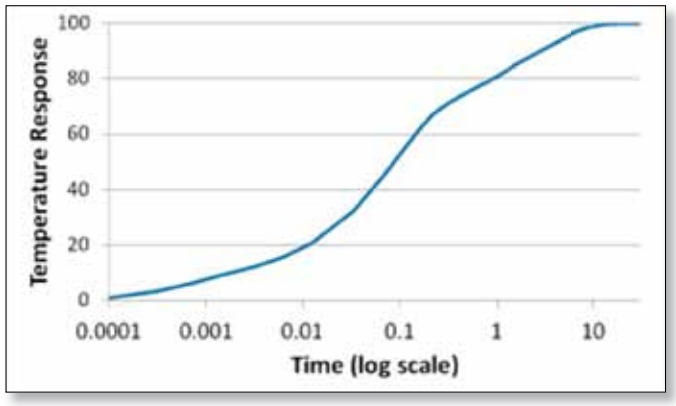

FIGURE 2b: Transient response (log time scale).

response represents a time history of the heated region to a step change in power. Since the system is linear, if only one-half of the heat load was applied, the time dependent curve could be scaled by a factor of 0.5 such that it would have reached a value of 50 at steady-state. While this was probably obvious to most readers, using this same information and superposition allows a prediction of the response to turning the power on and off to be made. As an example, suppose that the power was on for 0.5 units of time and off for 0.5 units of time and that this cycle repeated. Using the transient response in Figure 2, a periodic curve may be generated as the superposition of on and off responses. This is shown graphically in Figure 3. The on and off curves are time shifted so that the start of the curve coincides with

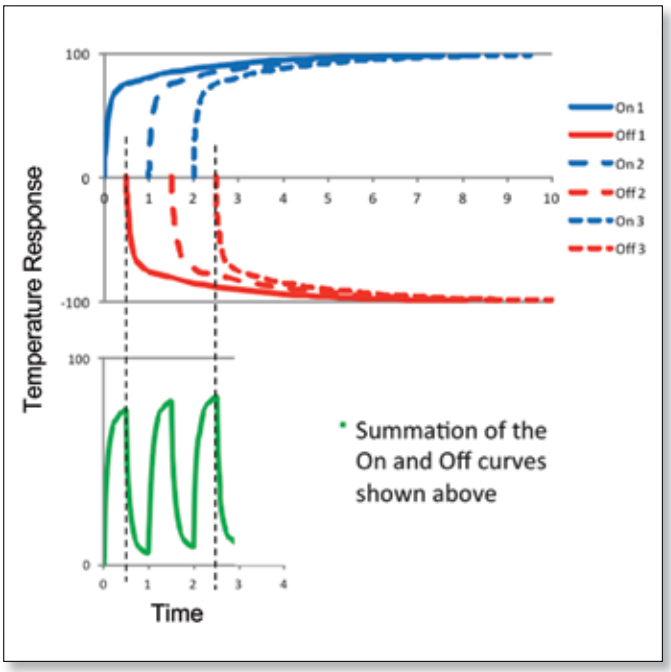

FIGURE 3: Superposition of transient response for an on/off condition.

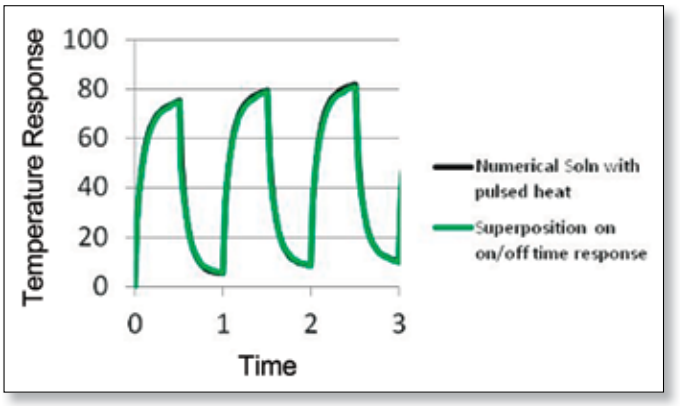

FIGURE 4: Comparison of superposition and numerical solution.

the start of a powered or off-state response. The response temperature is the summation of the time history of the responses that have occurred at a particular time value. For example, the response between 1 and 1.5 units of time is the summation of On 1, Off 1, and On 2.

As a check, the same simple model described in Figure 1 was modified to have the heat applied with the time profile (0.5 time units on and 0.5 time units off) and a comparison between the results is shown in Figure 4. The small difference between the two curves is a result of grid convergence in time, which brings up an additional benefit of superposition. It is often easier to do a time-step convergence study on a step-change response than it is on a cyclical power application case because of the need for small time steps where the system responds to an on or off application of the heat load.

A useful feature of this technique is that it is easy to generate the temperature response to different combinations of on and off cases and even different heat loads.

Note that the curve represented in Figure 2 did not necessarily need to be generated by a thermal model. The response could have been measured test data. Provided that the test data were a response to a step change in heat load and the system could be considered linear, the same superposition process would apply. A caution is in order using this technique, especially in systems with a large variation in time scales (such as features on an IC requiring time scales on the order of µsec coupled with other parts of the system that respond much slower such as seconds or minutes). In order to accurately use superposition, a complete time history curve to steady-state is required, and then care is required in the area of numerical precision because the response out at the later times is the summation of many preceding responses.

REFERENCES

[1] Guenin, B, "Power Map Calculations Using Image Sources and Superposition", ElectronicsCooling, Nov, 2008.

Malico Inc
5, Ming Lung Road, Yangmei, 32663 Taiwan
Tel: 886-3-4728155
Fax: 886-3-4725979
E-mail: inquiry@malico.com
Website: www.malico.com

www.malico.com

Metal Foam-PCM

Heat Storage Technology: The Thermal Charging Scenario

Nihad Dukhan and Sujay Bodke, Department of Mechanical Engineering
University of Detroit Mercy

Professor Dukhan is an Associate Professor of Mechanical Engineering at the University of Detroit Mercy, where he teaches courses in the thermal and fluids sciences. His technical research areas include novel thermal management solutions for high-power devices, with focus on metal foam. Professor Dukhan's publications include over 80 journal and conference papers. His edited book on metal foam will appear in June 2012. His research has been supported by Ford Motor Company, NASA, National Science Foundation, United Technologies and DENSO North America. Dr. Dukhan earned his Ph.D. in 1996 in Mechanical Engineering from the University of Toledo.

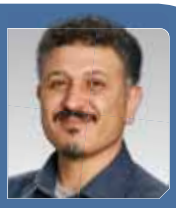

Sujay Bodke obtained his master's degree in mechanical engineering in 2010 from University of Detroit Mercy (UDM). At UDM he worked on projects related to the impact of emerging technologies on alternative energy, including hydraulic hybrid cars. He garnered the virtues of metal foam under the guidance of Dr. Dukhan. His professional career includes working for P3 North America, where he worked with various automotive OEM's for the development of telematics for electric vehicles. He is now working at Detroit Diesel as a consultant to plan and forecast engine prototypes to cut cost and help organize developmental work.

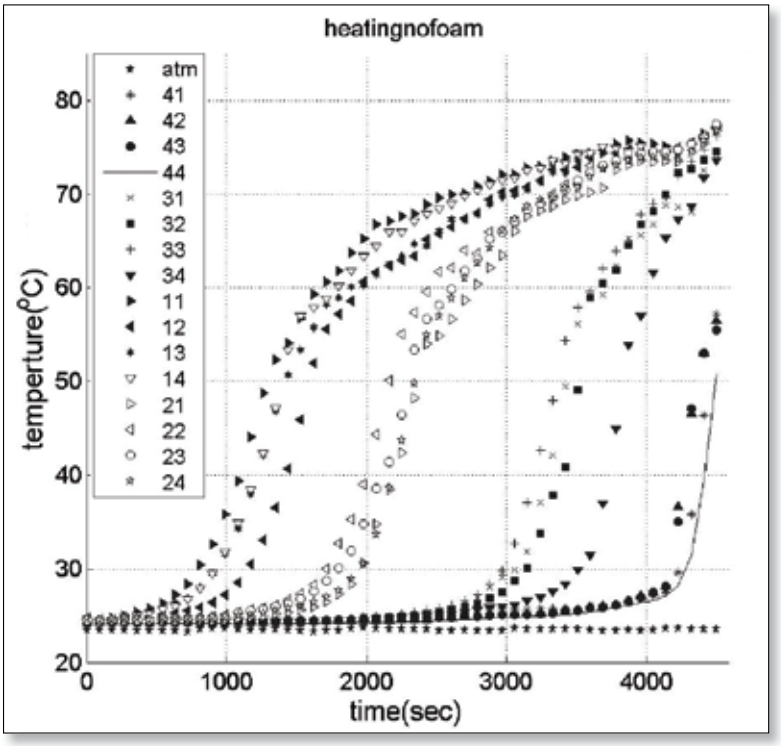

FIGURE 1: Heating patterns for wax only.

FOR OPTIMAL operation of electronics, the generated heat must be removed and hot spots must be mitigated. If the junction temperature increases above a specified limit, some electronic components may fail, or experience a decline in performance. Excess temperature also causes thermal stresses that lead to fracture of electronic packages.

Phase change materials (PCMs) are excellent for storing heat due to their high latent heat of fusion [1-3]. PCMs need higher conductivity to improve their performance [2,3].

Aluminum foam has low density, high thermal conductivity and interconnectivity [4]. Its applications include heat exchangers and lightweight structural components. A plate fin heat sink with the tip immersed in a PCM showed enhanced performance [5].

This brief discusses an experimental study of a thermal storage technology made by embedding aluminum foam in Paraffin wax, along with the resulting enhancements. Further details can be found in reference [6]. For some electronics devices under transient conditions, an increased thermal capacitance can limit temperature increases and/or reduce the cooling requirement of a heat sink. The combination of aluminum foam and PCMs can provide this thermal capacitance and furnish a nearly-isothermal heat sink while the PCMs are melting.

Introducing our answer to reducing data center energy costs: EcoBreeze

EcoBreeze uses two economizer modes of cooling depending on local weather and temperature conditions.

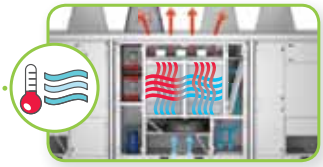

Air-to-air heat exchange:

Passes hot IT air into EC fans and then passes air through internal channels of a heat exchanger.

Indirect evaporative cooling:

Removes heat from IT air by evaporating water on the outside of the indirect evaporative cooler's heat exchanger channels.

Introducing the only modular, indirect economizer: EcoBreeze.

Data centers face unprecedented cooling challenges brought on by high-density computing, dynamic temperature profiles, regulatory requirements related to efficiency, and uncertain long-term plans for capacity or density. Today, Schneider Electric™ has the innovative answer to meeting these and other cooling challenges.

Introducing Schneider Electric EcoBreeze

EcoBreeze™ is the industry's only economizer with two economization modes in one footprint. Specifically, it automatically can switch back and forth between air-to-air heat exchange and indirect evaporative cooling to maximize local climate conditions at all times. As a result, it uniquely ensures the most efficient and effective form of cooling year round.

In addition, the innovative cooling solution boasts a modular design for capacity, redundancy, and service flexibility. What's more, scalable 50 kW modules make right-sized cooling possible, allowing data center operators to match cooling capacity to actual cooling needs. And EcoBreeze is much faster and easier to deploy than traditional data center cooling infrastructure.

Efficient, scalable, and flexible, EcoBreeze enables Business-wise, Future-driven™ data centers.

Business-wise, Future-driven.

- **Faster and easier:** Flexible, quick, and cost-effective deployment since unit used zero white space with the data center.
- **Right-sized:** The pre-engineered 50 kW modules that fit into two frame sizes can be scaled to 200 kW - 400 kW increments of capacity and redundancy requirements as needed, lowering both CapEx and OpEx.
- **Energy-efficient:** Automatically switches between air-to-air and indirect evaporative heat exchange for the most efficient cooling. A supplemental DX circuit on board gives additional peace-of-mind reliability.
- **Two economizer modes:** Indirect evaporative cooling and air-to-air heat exchange in the same module enable more economization opportunities.

Make the most of your energy℠

Economize with economizer modes! Maximize savings after reading "Economizer Modes of Data Center Cooling Systems" and enter to win an iPad® 2!

Visit www.SEreply.com Key Code n774v Call: 888-289-2722 x7271

Schneider Electric™

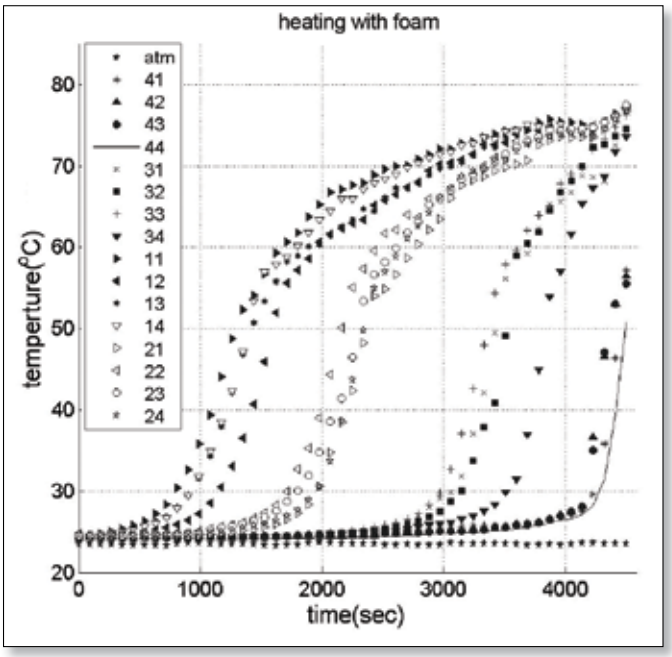

FIGURE 2: Heating patterns for wax with aluminum foam.

EXPERIMENT

The commercial foam used in this study was made from aluminum alloy 6101-T6 and had 4 pores per cm and 90% porosity. The paraffin wax used in this experiment had a melting temperature of 60 °C. Heating was provided by an electric heater attached to an aluminum plate of 0.63 cm thickness and a face size of 10.16 x 10.16 cm^2. A variac controlled the wattage that was supplied to the heater.

The wax and the foam/wax combination were contained in a wooden cavity having a depth of 10.8 cm and a cross-sectional area of 10.16 x 10.16 cm^2. Thermocouples were inserted at various depths in groups of four at 2.54, 5.08, 6.35 and 8.38 cm from the top, respectively. A data acquisition system recorded the temperatures.

A volume of 1048 cm^3 of wax was preheated to a temperature above its melting point and was poured into the wooden cavity. After cooling to ambient temperature, the bottom heater provided a constant heat input of 82.3 W. The temperatures were recorded every three seconds, until all the thermocouples readings were above the melting point of the wax.

With the wax in its liquid phase, a cube of foam with a side length of approximately 10.16 cm was inserted into it very slowly to avoid formation of air pockets. The foam had a porosity of 90 %. The foam/wax combination was allowed to cool to room temperature. The electric heater was switched back on and provided 82.3 W. The temperature of each thermocouple was recorded until the temperature of the uppermost thermocouple was above the melting point of the wax.

RESULTS

Figures 1 and 2 show the temperature profiles during the period of heating for the two cases. To understand the heating patterns, and to assess the enhancement due to foam addition, consider an imaginary vertical line along the time

	With Foam	Without Foam	Change
Heating time (hrs)	1.09	1.27	15.3%
Max. Temperature (°C)	68.0	79.0	10.5%

TABLE 1. Time and temperatures for wax and wax/foam combination.

2000 seconds in Figs. 1 and 2. At 2000 seconds, no-foam case temperatures ranged from 20 to 70 °C. This means that the top surface was still solid (at ambient temperature), while the wax at the bottom was liquid (above the melting point). The foam/wax heating temperature ranges from 33 to 54 °C. Thus, the temperature gradient for no-foam is almost twice greater than that of the with-foam case.

Table 1 gives the maximum temperature and the time required for the wax to melt for the two cases. The foam reduced the heating time by 15%, while the maximum temperature was 11% less than for no-foam heating.

CONCLUSION

The conductivity of paraffin wax was enhanced by combining it with aluminum foam. Heating curves at different locations were obtained experimentally for the wax alone and the wax/foam combination. The results proved that the inclusion of foam decreased the charging time by 15.3%, and the maximum temperature by 10.5%. The foam also improved the heat distribution in the wax, which made the temperature significantly more uniform during charging. For some electronics devices under transient conditions, the combination of aluminum foam and PCMs overcomes the issue of the low conductivity of PCMs and can provide an increased thermal capacitance which limits temperature increases and/or reduce the cooling requirement of a heat sink.

REFERENCES

[1] O. E. Ataer, "Storage of Thermal Energy," in Energy Storage Systems, Edited by Y. A. Gogus, in Encyclopedia of Life Support Systems, Eolss Publishers, Oxford, UK, 2006.

[2] A. Heinz and W. Streicher, "Application of Phase Change Materials and PCM-Slurries for Thermal Energy Storage," Institute of Thermal Engineering, Graz University of Technology, Austria, 2006.

[3] J. Wilson, "Phase Change Materials Thermal Properties," Electronics Cooling, Issue: May 1st, 2005.

[3] N. Dukhan, "Correlations for the Pressure Drop for Flow through Metal Foam," Experiments in Fluids, vol. 41, pp. 665-672, 2006.

[4] S. Krishnan, S. V. Garimella and S. S. Kang, "A Novel Hybrid Heat Sink Using Phase Change Materials for Transient Thermal Management of Electronics," IEEE Transactions on Components and Packaging Technologies, vol. 28, No. 2, pp. 281-289, 2005.

[5] N. Dukhan and S. Bodke, "An Improved PCM Heat Storage Technology Utilizing Metal Foam," Proceedings of IEEE iTherm Conference, Las Vegas, NV, June 2-5, 2010.

Designing Heat Sinks

When a Target Pressure Drop and Flow Rate is Known

Madhusudan Iyengar, Associate Editor

FORCED CONVECTION air cooled heat sinks and liquid cooled cold plates are quite pervasive in their use in electronics cooling applications. While there can be significant debate on whether to air or liquid cool a particular component, the approach a thermal engineer would adopt to design both components is essentially similar. Parallel plate fins are the most common geometry used to form the core structure of both devices. Simple hydraulic and thermal relationships from literature for plate fins and parallel plate ducts can be used for design. Often the first question that comes to mind before even starting a back of the envelope calculation for a heat sink or cold plate is: "What is the target volumetric flow rate and coolant pressure drop that we are designing towards?" The answer to this question is often determined from a high level system design that may estimate what the flow rate and pressure drop "budget" can be. It can also result from a choice of a fan that provides its user with a finite number of flow and pressure drop operating points. For air cooled heat sinks, another pertinent early question can be: "What is the volume available for this heat sink in the system?" This question may be less relevant for liquid cooled cold plates, because they are often extremely compact and small changes in their volume can usually be accommodated at the system level without too much difficulty.

It is often not obvious what geometry would satisfy target conditions for flow and pressure drop. This article will assume knowledge of target flow rate, pressure drop, and volume as design targets and will derive equations to allow thermal designers to design a heat sink or a cold plate to meet their needs. In this respect, this article differs from what has been previously published in this magazine [1], where the hydraulic and thermal performance of an assumed geometry was calculated. Although the previously presented calculations [1] can be and are often used, the methodology described herein could help designers converge more rapidly on geometries that match their specific needs.

Figure 1 shows a schematic of an array of plate fins attached to a base with coolant (air or liquid) flow through the channels between the fins. The heat input, q, is assumed to be uniform for simplicity, although spreading in the base from a discrete heat source can be easily calculated using previous articles [2, 3]. Figure 1 shows the width,

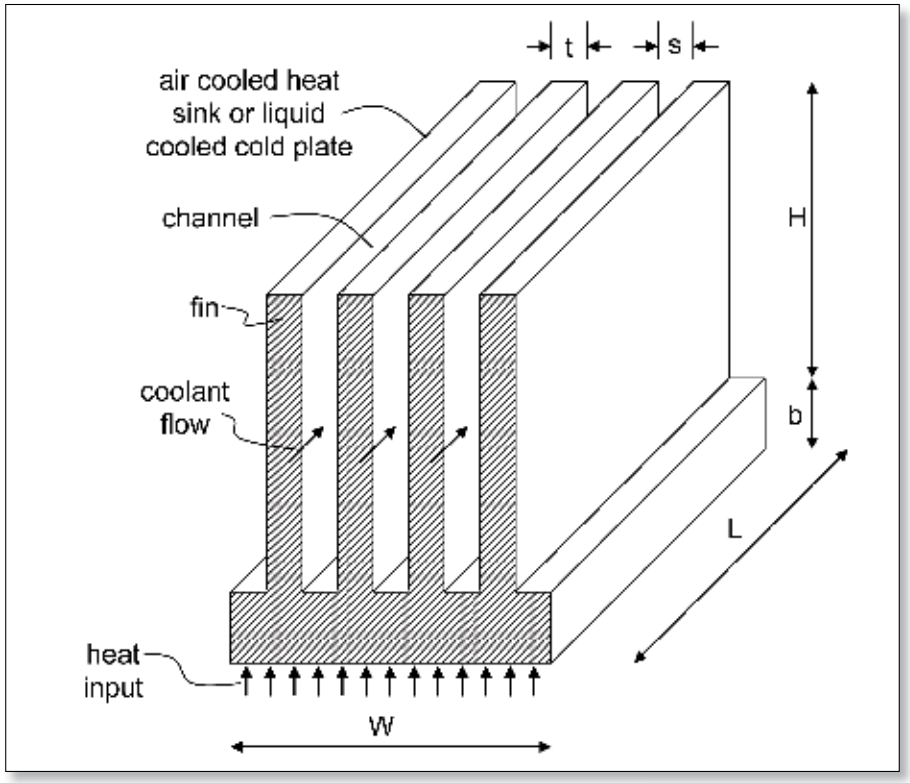

FIGURE 1: Schematic of a plate fin heat sink.

length, and height of the heat sink denoted as W, L, and H, respectively, and the fin thickness and channel spacing are represented by t and s, respectively. The thickness of the heat sink base is b. Flow bypass [4] is also not considered in this article. The analyses presented in this paper assumes the following:

- forced convection
- parallel plate heat sinks
- fully ducted flow
- fully developed laminar flow
- uniform heating of the heat sink base
- no entrance and exit effects
- equal number of fins and channels
- large aspect ratio for the channels
- high thermal conductivity fins
- uniform temperature on duct surface for Nusselt number estimation.

N	s mm	t mm	h_{cn} W/m^2-K	η	R °C/W
20	1.28	3.72	78.2	0.88	0.165
30	1.12	2.22	89.5	0.79	0.139
40	1.02	1.49	98.5	0.7	0.128
50	0.94	1.06	106.1	0.62	0.123
60	0.89	0.78	112.7	0.54	0.12
70	0.84	0.59	118.7	0.47	0.118
80	0.81	0.44	124.1	0.41	0.117

TABLE 1: Aluminum air cooled heat sink calculation.

Neglecting the entrance (contraction) and exit (expansion) pressure losses, the pressure drop across a fully ducted heat sink can be assumed to be comprised of only the frictional component, and estimated by [5],

$$\Delta P = f \times (L/D_h) \times (½) \times (\rho U^2) \quad (1)$$

where f, D_h, ρ and U are the Darcy friction factor, channel hydraulic diameter, fluid density, and channel flow velocity, respectively.

The Darcy friction factor is defined as a dimensionless pressure drop for internal flow [5], and for fully developed laminar flow between infinite parallel plate ducts, can be given by [6],

$$f = 96/Re \quad (2)$$

where Re is the Reynolds number which is computed using,

$$Re = \rho U D_h/\mu \quad (3)$$

where μ is the fluid dynamic viscosity.

While the hydraulic diameter for ducts is defined as the ratio of four times the duct cross-sectional area to the duct perimeter, it can be approximated for high aspect ratio ducts to be,

$$D_h = 2s \quad (4)$$

The channel velocity U is the ratio of the flow rate to the duct cross-sectional area, and is given by,

$$U = V/NHs \quad (5)$$

where V is the coolant volumetric flow rate and N is the number of channels. The denominator in eq.(5) is the duct cross-sectional area.

Substituting eqs. (2)-(5) into eq.(1), we get,

$$\Delta P = (12\mu LV)/(s^3NH) \quad (6)$$

Since, we are assuming knowledge of the target design pressure drop to converge on the desired fin geometry, we can express eq.(6) as,

$$s = [(12\mu LV)/(\Delta PNH)]^{⅓} \quad (7)$$

After calculating the channel spacing that meets our needs, the fin thickness can be given by,

$$t = (W-Ns)/N \quad (8)$$

Eq. (8) does assume that there are equal number of fins and channels which is a reasonable assumption when there are many fins and channels.

The dimensionless Nusselt number is often used to characterize heat transfer in channels, and is given by,

$$Nu = h_{ch}D_h/k_f \quad (9)$$

where h_{ch} and k_f are the channel heat transfer coefficient and fluid thermal conductivity, respectively.

Using the assumption of fully developed laminar flow in narrow ducts, the Nusselt number given by eq.(9) has been found to be 7.541 [6] for uniform temperature duct surfaces. Thus, by rearranging the terms in eq.(9), using eq.(4) and the value of 7.541 [6] for the Nusselt number, we can calculate the channel heat transfer coefficient as,

$$h_{ch} = 3.8\ k_f/s \quad (10)$$

In order to calculate the thermal performance of this array, we need to calculate the fin efficiency, which can be given by [5],

$$\eta = \tanh(mH)/(mH) \quad (11)$$

where m is fin parameter which is calculated using,

$$m = (2h_{ch}/kt)^{0.5} \quad (12)$$

where k is the thermal conductivity of the fin material.

The thermal resistance of the uniformly heated heat sink (or cold plate), R, can be formulated as,

$$R = R_{conv} + R_{cal} + R_{base} \quad (13)$$

where R_{conv}, R_{cal}, and R_{base} are the convective, the caloric sensible coolant temperature rise, and the base 1-D conduction, components of the thermal resistance, respectively.

Eq. (13) can be further expanded to be expressed as,

$$R = 1/(h_{ch}NL(2\eta H+s)) + 0.5/\rho C_pV + b/kLW \quad (14)$$

where C_p is the fluid specific heat.

It should be noted that there exist other ways to construct a total thermal resistance as detailed in [7, 8] in which the heat sink surface is assumed to be at a uniform temperature. Under such an assumption, the caloric thermal resistance term ($0.5/\rho C_pV$) provided in eq.(14) would be replaced by a different term that accounts for a non-linear coolant temperature rise as it passes through a duct whose surface is at a uniform temperature. The term for the caloric thermal resistance in eq. (14) assumes that the uniform base heat flux would result in a linear coolant temperature along the length of the heat sink.

The important equations from the preceding analytical treatment that can be used by the thermal designer are eqs. (7), (8), (10), (11), and (14) which can lead to the calculation

of thermal resistance for a heat sink design that would satisfy flow rate and pressure drop targets. In addition, the designer would have to specify a fin material (e.g. copper or aluminum), a coolant (e.g. air or water), a heat sink volume (L, W, H), the base thickness (b), and the number of channels (N). The last parameter, N, can be changed parametrically to yield multiple designs that satisfy the target constraints, and a design can be chosen based on the thermal resistance (R) as well as what fin thickness and channel spacing are manufacturable.

N	s mm	t mm	h_{cn} W/m^2-K	η	R °C/W
20	0.29	0.96	8136	0.99	0.136
25	0.27	0.73	8764	0.98	0.109
30	0.25	0.58	9313	0.97	0.092
35	0.24	0.48	9805	0.97	0.081
40	0.23	0.4	10251	0.96	0.072
45	0.22	0.34	10661	0.95	0.066
50	0.21	0.29	11042	0.94	0.062
55	0.2	0.25	11399	0.93	0.058
60	0.2	0.22	11734	0.92	0.055

TABLE 2: Copper water cooled cold plate calculation.

Table 1 shows results of such calculations for designing an air cooled aluminum heat sink that meets a target of 50 Pa at 0.0047 m^3/s (10 cfm), for a fin array volume of 100 mm (L) by 100 mm (W) by 50 mm (H). For the results shown in Table 1, the base is assumed to be 5 mm. The channel number, N was varied from 20 to 80 to yield the results shown in Table 1, which result from the sequential use of eqs. (7), (8), (10), (11), and (14).

If the target heat load is 160 W at a heat sink base to inlet air temperature difference of 20 °C, then the target thermal resistance would be 0.125 °C/W. As seen from Table 1, the 50 fin design would yield such a design point. Such a heat sink would meet the target flow conditions and would comprise of 1.06 mm thick fins that are spaced 0.94 mm apart. Thus, both required cooling performance and heat sink manufacturability [9] would have to be considered in arriving at a desired design. If the manufacturable designs cannot provide the required cooling, then one or more of the target conditions may have to be changed. For example, the flow and pressure drop may need to be higher or the volume may be increased or a different fin material could be considered. Since the base thickness and volumetric flow rate is fixed for all the designs displayed in Table 1, they yield constant 1-D base conduction and caloric thermal resistances of 0.002 °C/W and 0.091 °C/W, respectively.

Table 2 shows a similar analyses as was discussed in the preceding text, but for a water cooled copper cold plate that is 25 mm (L) by 25 mm (W) by 1 mm (H) with a target flow rate of 6.308 x 10^{-6} m^3/s (0.1 gpm) at 3447 Pa (0.5 psi). The base is assumed to be 2 mm. If the target heat load is 320 W with an available temperature excess of 20°C between the cold plate base and the inlet water, then the target thermal resistance would be 0.0625 °C/W. As can be seen from Table 2, a design using 50 fins with 0.29 mm thick fins spaced 0.21 mm apart would yield a thermal resistance of 0.0625 °C/W. Since the base thickness and volumetric flow rate is also fixed for all the designs displayed in Table 1, they yield constant 1-D base conduction and caloric thermal resistances of 0.008 °C/W and 0.019 °C/W, respectively.

It should be noted that the assumption of the 7.541 value for the fully developed laminar flow Nusselt number is good for very high aspect ratio (H/s) ducts. For smaller aspect ratios, such as 8 for example, this value is much lower (5.6) [5]. This effect can, if needed, be included into eq. (10) with an addition of an aspect ratio term, but has been left out for simplicity in this article. Also, the value of 7.5 is for a uniform temperature on the duct channel surface and the

uniform heat flux boundary condition value is a bit higher (8.23) [5]. In reality, the boundary condition is neither a constant heat flux nor a constant temperature one.

Several other assumptions have been made in the calculations presented in this article. The objective has been to provide a rapid method to converge on some feasible geometries that address a target design point. For a specific design, it may be required to subsequently perform a full numerical analysis (CFD) or consider aspects such as entrance and exit pressure losses, the influence of the channel aspect ratio on the fully developed laminar Nusselt number, flow regime (laminar versus turbulent), the impact of developing flow, and the use of a precisely calculated hydraulic diameter. In addition to the heat sink calculation performed herein, one would of course need to calculate the bypass flow (if any), the spreading resistances (lid to heat sink base or at the chip hot spots) as well as the thermal resistance of all the thermal conduction layers between the heat sink base and the chip junction. In closing, even though this calculation corner provided numerical values to several digits, we should remember that the end result is only an estimate as mentioned in the first paragraph.

REFERENCES

[1] R. Simons, "Estimating Parallel Plate-Fin Heat Sink Thermal Resistance," Electronics Cooling, February, 2003.

[2] S. Lee, "Calculating Spreading Resistance in Heat Sinks," Electronics Cooling, January, 1998.

[3] R. Simons, "Simple Formulas for Estimating Thermal Spreading Resistance," Electronics Cooling, May, 2004.

[4] R. Simons, "Estimating the Effect of Flow Bypass on Parallel Plate- Fin Heat Sink Performance," Electronics Cooling, February, 2004.

[5] F. P. Incropera, and D.P. Dewitt, "Introduction to Heat Transfer," 2nd Edition, John Wiley and Sons, 1990.

[6] W. M. Rohsenow, J.P. Hartnett, and Y.I. Cho, "Handbook of Heat Transfer," 3rd Edition, McGraw-Hill, 1998.

[7] R. Simons, "A Simple Thermal Resistance Model – Isoflux Versus Isothermal," Electronics Cooling, February, 2006.

[8] R. Moffat, "Modeling Air-Cooled Heat Sinks As Heat Exchangers," Electronics Cooling, February, 2008.

[9] M. Iyengar and A. Bar-Cohen, "Design for manufacturability of Forced Convection Air Cooled Fully Ducted Heat Sinks," Electronics Cooling, August, 2007.

SEMI-THERM®

Thermal Innovations for a Cool World
Semiconductor Thermal Measurement, Modeling and Management Symposium
T W E N T Y - N I N T H A N N U A L

CALL FOR PAPERS

March 17-21, 2013
DoubleTree Hotel, San Jose, CA, USA

The conference

SEMI-THERM is an international forum dedicated to the thermal management and characterization of electronic components and systems. It provides knowledge covering all thermal length scale from IC level to applications. The symposium fosters the exchange of knowledge between thermal engineers, professionals and leading experts from industry as well as the exchange of information on the latest academic and industrial advances in electronics thermal management. Since 2012, SEMI-THERM includes a **dedicated datacenter cooling track**. The forum is sponsored by IEEE, CPMT, and NIST. Areas of interest include, but are not limited, to the following:

Topics:

- Practical Thermal Solutions for Low-Cost, High-Volume Systems Design
- Package Thermal Design and Components for High-Volume Semiconductor Packages
- System-Level and Board-Level Thermal Design
- Multidisciplinary approach and solutions for thermal management and energy reduction
- Solutions for Harsh Environments in Commercial, Defense, and Aerospace Systems
- Thermal Solutions for specific Environments like low noise, etc
- Characterization and Standardization of Material Property Measurements
- Thermal Integration in the Product Design Process
- Characterization and Modeling of Thermo-Mechanical effects
- Characterization and Modeling of multi-scale heat transfer problems
- Characterization and Modeling of Components, Boards and Systems
- Multi-physics modeling and characterization of product or process
- Novel approach for analysis and Modeling
- CFD Analysis of Complex Geometries and Validation
- Temperature and Thermal Property Measurement Techniques
- Transient Thermal Control Methodologies
- Novel and advanced cooling techniques/technology or temperature control
- Compact Modeling, Model Reduction and Validation
- Roadmaps, Specifications and Traditional Cooling Limits

Application areas:

- Processors, ICs, and Memory
- Alternative and Renewable Energy
- LED lighting
- Data Center
- Computing systems
- Portable and Consumer Electronics
- Power Electronics
- Harsh Environments
- Defense and aerospace
- Medical and Biomedical
- Instrumentation and controls
- Accelerated Testing
- Solid state energy generation/cooling

Conference highlights

- Two days of short courses will be offered (17th - 18th March 2013). Topics will be confirmed at a later stage.
- Vendor exhibits from suppliers of cooling technologies, experimental characterization equipment, and computer simulation software
- Technical workshops, tutorials, sessions

To submit an abstract

You are invited to submit an extended abstract describing the scope, contents, key results, findings and conclusions. This abstract of 2 to 5 pages is supported by figures, tables and references as appropriate. **Abstracts must demonstrate high technical quality, originality, potential impacts. Upload your abstract electronically** in RTF, DOC or PDF formats at www.semi-therm.org

Abstract Deadline	Abstract Acceptance Notification	Photo-ready Full Manuscript Due
August 31, 2012	November 1, 2012	January 3, 2013

SEMI-THERM actively solicits student papers and awards travel stipends and reduced conference fees.
The best papers may be invited to be published in *IEEE Transactions on Components and Packaging Technologies.*

For further information please contact the Program Chair:
Genevieve Martin, Philips Research, E-mail: genevieve.martin@philips.com , Phone: (+31) 40 27 49199
Visit our website: http://www.semi-therm.org

Modeling and Experimental

Characterization of Hot Spot Dissipation in 3D Stacks

Herman Oprins, Vladimir O. Cherman, Imec, Leuven, Belgium

Herman Oprins received the M.Sc and Ph.D. degrees in Mechanical Engineering from the K.U.Leuven in 2003 and 2010 respectively. He joined Imec in 2003, pursuing the PhD degree on the development and modeling of an electrowetting assisted cooling technique in collaboration with the K.U.Leuven and working on modeling and experimental projects on thermal management of electronic packages. Currently he is working as senior research engineer in Imec, where he is involved in the thermal experimental characterization, thermal modeling and thermal management of 3D-ICs, electronic packages, GaN transistors, photovoltaic modules and microfluidics.

Vladimir O. Cherman received his M.Sc and Ph.D degrees in electronic engineering from Saint-Petersburg Electrotechnical University (LETI) Russia, in 1994 and 1999, respectively. From 1997 to 2000, he was with Morion Inc. St.-Petersurg, Russia as an electronics engineer. From 2000 to 2007 he was with Ceramics Laboratory at Swiss Federal Institute of Technology-Lausanne (EPFL) where his research was focused on microwave properties of ferroelectric materials. He joined the Reliability and Modeling group of Imec as a researcher in 2007, where he is involved in reliability study of MEMS devices and electronic packages.

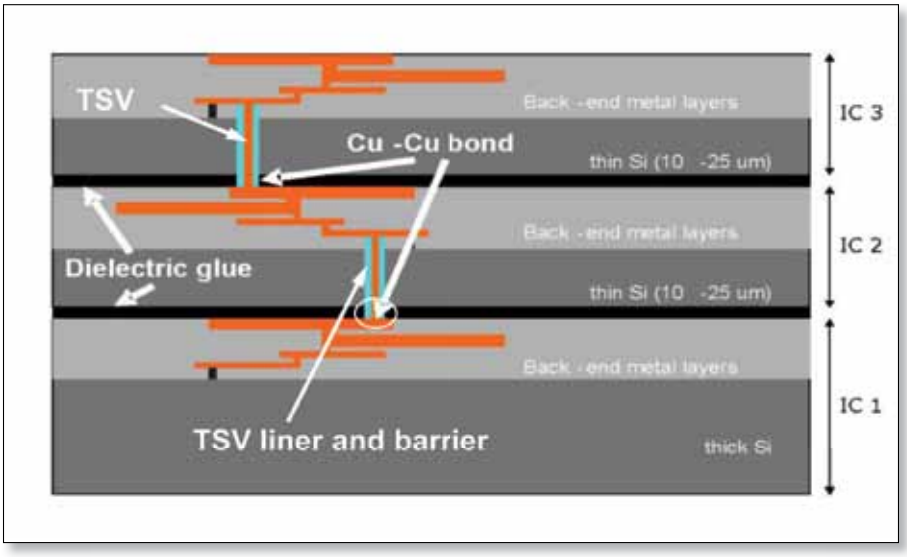

FIGURE 1: Schematic cross section of the 3D-integration using through-Silicon vias (TSVs).

THREE-DIMENSIONAL (3D) integration is considered a very promising technology for integrated circuit design [1]. It offers numerous opportunities to designers looking for more cost-effective system chip solutions. It allows further decrease in the form factor of today's systems and eases the interconnect performance limitation since the components are integrated on top of each other instead of side-by-side, resulting in shorter interconnect lengths. Furthermore, it makes it possible to interconnect multiple heterogeneous chips, and with much higher I/O density than in today's packaging solutions [2]. Thermal management issues in these 3D stacks are considered to be one of the main challenges for 3D integration [3]. The use of polymer adhesives with low thermal conductivity, the vertical integrations of the chips and the reduced thermal spreading due to aggressively thinned dies cause these thermal management issues. The presence of interconnection structures, back end of line (BEOL), redistribution layers (RDL) and through-Si vias (TSVs) increases the complexity of the conductive heat transfer paths in a 3D stack. To understand the effect of these TSVs and inter-tier connections, a detailed analysis of the heat transfer in 3D stacks, including the TSVs is needed.

This article focuses on the hot spot power dissipation in two-die stacks. The impact of TSVs and the Cu-Cu bonding on the temperature profile of

FloTHERM ▪ FloEFD ▪ FloVENT ▪ T3Ster

FloTHERM® 3D CFD SOFTWARE. From the smallest electronics such as LEDs and PCBs to a data center full of server racks, Mentor Graphics FloTHERM, a powerful 3D computational fluid dynamics software package, helps you create better products faster. FloTHERM is the CFD solution for electronics cooling applications. Find out how by downloading our whitepaper, "Beer Fridge: A Personal Journey", at www.mentor.com/go/beer-fridge

Mentor Graphics®
THE EDA TECHNOLOGY LEADER

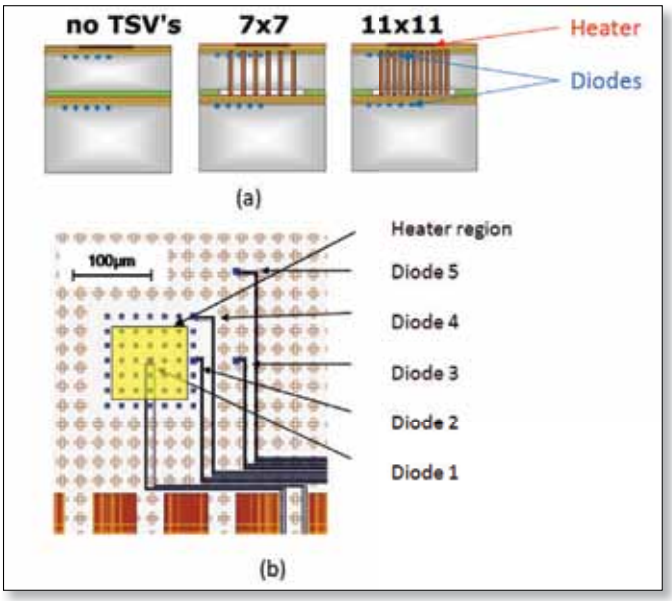

FIGURE 2: (a) Schematic cross-section of the die stack at the location of the test structures, revealing the TSV array density. (b) Detail of the design layout showing the heater, diodes and TSV array.

the top and bottom die is studied by using dedicated test structures consisting of integrated thermal heaters and temperature sensors. Die stacks including these structures are used to calibrate the thermal finite element modeling of the temperature distribution in the 3D stack.

THERMAL TEST VEHICLE FOR 3D STACKS

Dedicated test chips with integrated thermal structures are used to mimic power dissipation of a real chip and, at the same time, monitor the temperature at different locations in the stack. The 5x5 mm^2 top die is thinned down to 25 µm, to expose the 5µm TSVs at the backside; the top die is then stacked face-up on the 8x8 mm^2 bottom dies contained in the full thickness (725µm) landing wafer using Cu-Cu thermo-compression bonding [4] resulting in a typical stand-off height of 700 nm to 1 µm between the chips, shown in Figure 1. Cu meander heaters in the BEOL with sizes of 50x50 and 100x100 $µm^2$ respectively are used to dissipate power, and integrated diodes in both top and bottom die are used as temperature sensors. The temperature sensitivity of the diode is -2 mV/°C in the temperature range of 20 to 80 °C. Using a low current of 10 µA, power dissipation of the diode itself is negligible with respect to the power dissipated in the heaters. At the position of each heater, a set of 5 diodes at different distances (0, 60, 80, 120 and 160 µm respectively) from the hot spot center is added to both the top and bottom chip in order to capture the local temperature peak, and to monitor the vertical heat conduction in the stack. Furthermore, different TSV densities are used in the test chip, locally below the heaters to characterize their ability to enhance the heat transfer: a reference structure without TSVs, an array of 7x7 and 11x11 TSVs. Figure 2(a) shows a schematic representation of the cross-section of the test structures. In Figure 2(b), a detail of the layout at the location of a test structure is shown to reveal the location of the heater, diodes and TSV array.

Figure 3 shows a schematic cross section and a picture of the 2-level PCB that is used to provide the connections to the heaters and diodes. Four-point measurements are used both for the power dissipation and the temperature measurements. A Cu plate is glued to the backside of the PCB while the backside of the Cu plate is attached to a temperature-controlled, water-cooled heat sink. The chip stack under test is mounted on this Cu plate using a thermal interface material (TIM) and the chip stack is electrically connected to the PCB by wirebonds. The top side of the chip stack is thermally insulated, forcing the heat generated in the top die of the stack to be removed through the bottom side, to the heat sink.

THERMAL MODELING

Different thermal modeling approaches can be used to predict the thermal impact of TSVs and the Cu-Cu bonding in 3D-ICs at different stages of the design process. These approaches range from fast solving first order thermal calculations in the initial stage of the design [5,6], up to a detailed fine grain simulation including all layout details for the final verification of the design [7,8]. The FEM approach provides sufficient detail by allowing to include individual TSVs in the thermal analysis, while the computational time is sufficiently low to allow transient analysis. A parameterized finite element model representing the stack has been

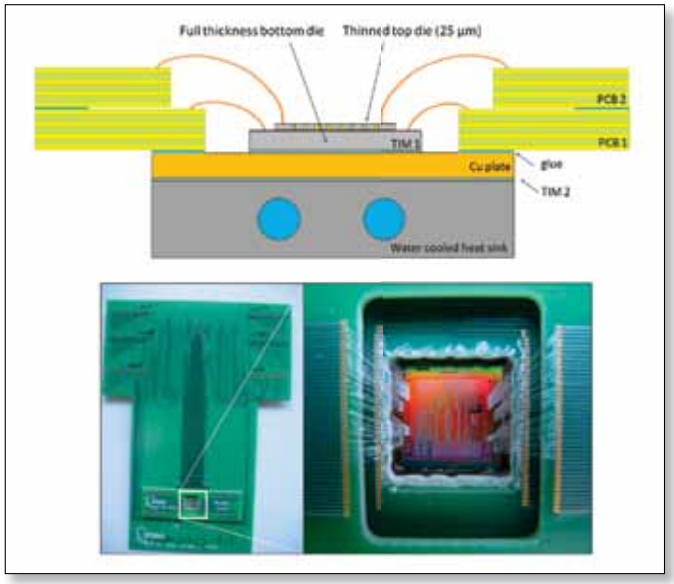

FIGURE 3: Top: Schematic cross-section of the test vehicle. Bottom: (left) Picture of the 2-level PCB. (right) Detail of the cavity in the PCB containing the die stack to reveal the wirebond connections from the PCB to the top and bottom die of the 3D stack.

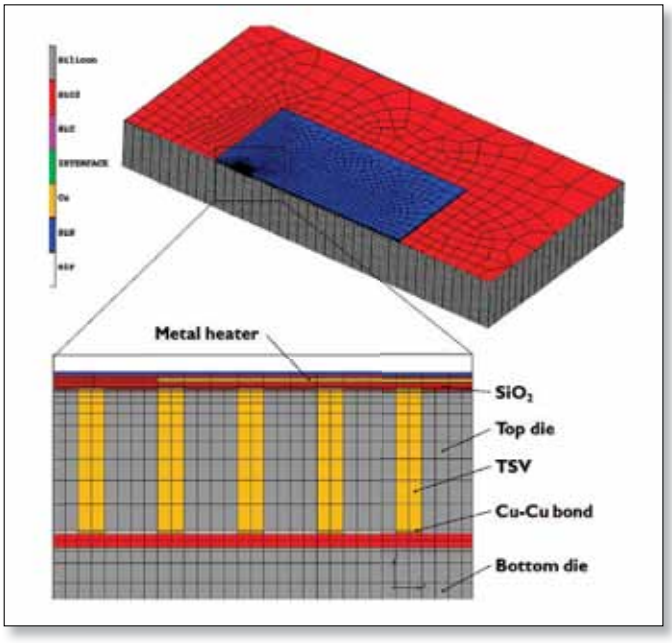

FIGURE 4: Top: 3D finite element model of the die stack. Bottom: Detail of the TSVs through the top die and the Cu-Cu bond to the bottom die.

constructed using a commercial software package [9]. Figure 4 shows a cross section of the model of the two-die stack. As boundary conditions, a heat flux represents the power dissipation in metal meander heaters. At the bottom of the die stack, an equivalent thermal resistance mimics the connection of the die stack to the Cu plate. The temperature distribution in the stack has been studied for the 6 different test structures on the test chip.

THERMAL COMPARISON OF 2D VERSUS 3D INTEGRATION

The 2D reference case is a full thickness die containing the integrated heaters and temperature sensors, whereas in the 3D case, the heaters are in the thinned top die, stacked on top of a full thickness bottom die. Figure 5 shows the experimental and modeling results for the temperature profiles in case of the test structure without TSVs for a power density of 12 W/mm^2 in the hot spots for the 2D and 3D case. For the experimental results, the error bars for the 95% confidence intervals based on the student's t-distribution are shown for 10 die stacks. The local temperature increase in the case of the 3D configuration is two to three times higher compared to the 2D reference case. Besides an increase in peak temperature, also a broadening of the temperature peak can be

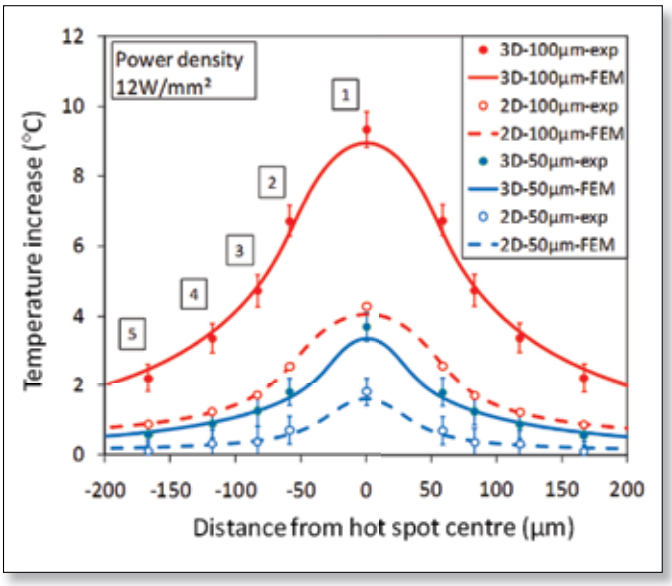

FIGURE 5: Temperature profile simulation (solid lines) and experimental (markers and error bars) results for a power dissipation of 12 W/mm² in 100x100 µm² and 50x50 µm² heaters in the 2D and 3D configuration.

observed. The normalized peak temperature is 82 K/W and 125 K/W for the 100x100 µm² and 50x50 µm² respectively. The measurement results indicate that the diodes are capable of capturing the local temperature peak below the hot spots. Furthermore, from this figure a good agreement between the modeling and experiments is observed.

THERMAL IMPACT OF TSVS

The simulations predict a local temperature reduction for an increasing TSV density compared to the no TSV case. A reduction of the local temperature increase of 7% and 20% is predicted for the 7x7 array and 11x11 array respectively. This is shown by the dashed lines in Figure 6(a) for the 100µm heater. However, a temperature increase (7x7 array) and a less than predicted temperature reduction (11x11 array) have instead been observed experimentally in all 10 chips. A detailed FIB-SEM analysis of the cross-section of the die-die interface revealed non-connected TSV in the outer ring of the arrays, slight variations in the stand-off height and non-uniform distribution of the polymer adhesive. The finite element model has been updated by taking into account these deviations from the designed geometry. The updated simulation results are able to correctly predict the expected impact of TSVs density (solid lines in Figure 6a). This analysis shows that the thermal impact of the die-die interface (adhesive, metal bond or voids) is at least as important as the impact of the TSVs for these stacks with a stand-off height from 700nm to 1µm. In the case of Cu or CuSn microbumps, the stand-off height is typically in the order of a few tens of µm and a larger thermal impact of the vertical die-die connection compared to the impact of TSVs is expected.

A transient analysis has been performed using a temporal resolution of 10 µs, which is sufficient to capture the fast temperature rise. From these measurements, the time constants for the temperature response are 100 µs and 200 µs for the top and bottom die, respectively. This is much faster than the transient response for uniform heating, for which a time constant of about 1s is typical. Figure 6(b) shows the comparison between the simulations results from the updated model and the experiments for the 100x100 µm² heater. For the 7x7 array a reduced vertical heat transfer (higher top die temperature, lower bottom die temperature) is observed. Due to the presence of non-connected TSVs, locally a larger fraction of the heat travels horizontally away from the heat source before travelling vertically towards the heat sink. The negative thermal effect of the non-connected TSVs dominates the positive effect of the added vertical connection with high thermal conductivity whereas in the case of the 11x11 array the positive effect of the high density array of TSVs is larger than the negative impact of the non-connected TSVs.

The calibrated thermal models for the two die stack are integrated [10] in an early physical design exploration flow, a.k.a. PathFinding flow [11]. This coupling of thermal and mechanical models to the design flow allows optimization of the design of stacked chips, as well as fine tuning stacking technology options, including TSV and microbump layout, for minimizing thermal and mechanical stress. The purpose of

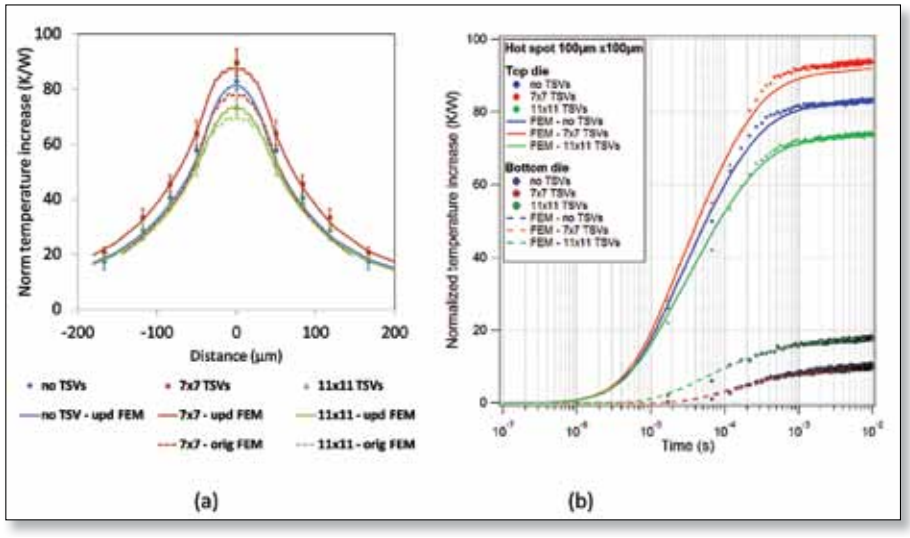

FIGURE 6: (a) Comparison of the temperature profiles simulated by the thermal model and the experimental results for the 100 µm x 100 µm heater. (b) Transient evolution of the peak temperatures (central diode 1) for the different TSV densities for the top and bottom die in case of the 100 µm x 100 µm heater.

the PathFinding is to validate product ideas for 3D, including the thermal and mechanical consequences, in the early phases of system design, before any large investments are needed.

CONCLUDING REMARKS

This article presents the thermal impact of TSVs and Cu-Cu bonding in 3D-ICs using finite element simulation and dedicated thermal test chips with integrated hot spot heaters, sensors and TSVs. Hot spot power dissipation results in significantly higher temperatures in 3D stacked chips compared to the same power dissipation in single 2D chips. This temperature increase is mainly due to the reduced thermal spreading in the thinned dies on the one hand, and to the use of adhesives with low thermal conductivity for the vertical integration of the chips on the other hand. Therefore, a detailed thermal analysis of the packaged 3D-IC is required and the conventional cooling solution used for the 2D chip might not be sufficient for the cooling of the 3D chip package. To limit the temperature increase in 3D-ICs, too thin chips should be avoided. Indeed, the thinner the silicon substrate, the higher the thermal spreading resistance is in the case of hot spots [12]. Simulations, used to extrapolate the experimental results of the 25 µm thick test chip for other thickness values, show that a minimum die thickness of 50 µm is required to deal with the local hot spots on the presented thermal test chip.

The study on the impact of TSVs on the temperature profile in the test chips shows that the thermal impact of the presence of the die-die connections, such as Cu or CuSn microbumps or direct Cu-Cu bonds, is more important than the presence of the TSVs itself. The Cu TSVs with high thermal conductivity (390 W/mK) are inserted in the Si, which is well conductive (150 W/mK at room temperature and120 W/mK at the operating temperature). Typical conductivity values for the underfill materials are 0.2 W/mK for unfilled underfills and 0.3-0.4 W/mK for filled underfills, depending on the amount and type of filler particles. The difference in thermal conductivity between the metallic bonds and the adhesive material is thus two orders of magnitude. As a result, well placed dummy microbumps, rather than dummy TSVs, can be used to increase the effective thermal conductivity and to reduce the temperature increase in a 3D stack.

REFERENCES

[1] Chanchani, R. "3D Integration Technologies – An Overview," in Materials for Advanced Packaging edited by D. Lu, C.P. Wong, Springer (2009), pp. 1-50.

[2] Beyne, E. "Through-Silicon via Technology for 3D IC," in Ultra-thin Chip Technology and Applications, edited by J.N. Burghartz, Springer (2011).

[3] Brunschwiler, T.; Michel, B. "Thermal Management of Vertically Integrated Packages," in Handbook of 3D Integration: Technology and Applications of 3D Integrated Circuits, edited by P. Garrou, C. Bower and P. Ramm. Wiley-VCH Verlag GmbH (Weinheim, 2008) Vol. 2, Part IV, pp. 635-649.

[4] Swinnen, B.; Jourdain, A. ; De Moor, P. ; Beyne E. Chapter in Wafer Level 3-D ICs Process Technology; edited by S. Tan, R.J. Gutmann, and L.R. Reif (Eds), Springer, 2008.

[5] Sridhar, A.; Raj, A.; Vincenzi, A.; Ruggiero, M.; Brunschwiler, T.; Atienza. D. "3D-ICE: Fast compact transient thermal modeling for 3D-ICs with inter-tier liquid cooling," ICCAD 2010, San Jose, CA, USA.

[6] Torregiani, C.; Oprins, H.; Vandevelde, B.; Beyne, E.; De Wolf, I. "Compact thermal modeling of hot spots in advanced 3D-stacked structures," Proc. EPTC 2009, pp. 131-136.

[7] Melamed, S.; Thorolfsson, T.; Srinivasan, A.; Cheng, E.; Franzon, P.; Davis, W.R. "Investigation of tier-swapping to improve the thermal profile of memory-on-logic 3DICs," Therminic 2010, Barcelona, Spain, 6-8 Oct. 2010.

[8] Oprins, H.; Srinivasan, A.; Cupak, M.; Cherman, V.; Torregiani, C.; Stucchi, M.; Vandevelde, B.; Van der Plas, G.; Marchal, P. and Cheng, E. "Fine grain thermal modelling and experimental validation of 3D-ICs," Microelectronics Journal, Vol. 42 (4), April 2011, pp. 572-578.

[9] MSC.Marc, URL: http://www.mscsoftware.com/Products/CAE-Tools/Marc.aspx

[10] Milojevic, D.; Oprins, H.; Ryckaert, J.; Marchal, P.; Van der Plas, G. "DRAM-on-logic Stack – Calibrated thermal and mechanical models integrated into PathFinding flow," IEEE Custom Integrated Circuits Conference (CICC), 2011.

[11] Milojevic, D.; Varadarajan, R.; Seynhaeve, D.; Marchal, P. "PathFinding and TechTuning," in Three Dimensional System Integration, Springer (2011), pp. 137 – 186.

[12] Lasance, C. "Thermal Facts & Fairy Tales: Heat Spreading Revisited," Electronics Cooling, March 2012.

Spray Cooling

Heat Transfer - Test and CFD Analysis

Charles R. Ortloff, Marlin Vogel, CFD Consultants International, Ltd.

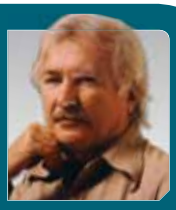

Charles R. Ortloff is currently director of CFD Consultants International, Ltd. and formerly Manager of the Applied Mechanics Department at BAE Systems, United Defense Corporation and FMC Corporation's Corporate Technology Center in Santa Clara and with prior Senior Engineer positions at GE Nuclear, Defense Research Corporation and Aerospace Corporation. He conducted research and development activity for the defense, nuclear, chemical, petroleum, ocean engineering and energy conversion industries over many years. With interests in the history of technology and archaeology, Charles is a Research Associate in Anthropology at the University of Chicago with B.Ae.E., M.Ae.E. degrees from NYU/Polytechnic in Aeronautical Engineering, a Ph.D. in the history of technology and Ph.D. studies in physics, fluid mechanics and mathematics at UCLA. Charles is the author of the Oxford Press book "Water Engineering in the Ancient World: Archaeological and Climate Perspectives on Ancient Societies of South America, the Middle East and South East Asia" and the author of 75 journal papers in engineering and archaeological journals with numerous book articles and television documentaries related to archaeological work around the world.

Marlin Vogel is presently a Distinguished Engineer at Juniper Networks, where he has led cooling technology roadmap development since 2010. Marlin was a Sr. Staff level engineer at Sun Microsystems where he conducted research, development, and productizing thermal technologies for CPU applications for 18 years, beginning in 1991. Marlin was a member of the General Dynamics Thermodynamics Analysis group for 7 years prior to joining Sun Microsystems, serving as co-leader of the thermal design for Navy stealth jet aircraft engine exhaust. Marlin obtained his Mechanical Engineering degree in 1979 and his M.S. degree in 1984 from the University of Wisconsin – Milwaukee and has authored over 25 publications on electronic cooling, and has been awarded 13 patents on electronic cooling inventions.

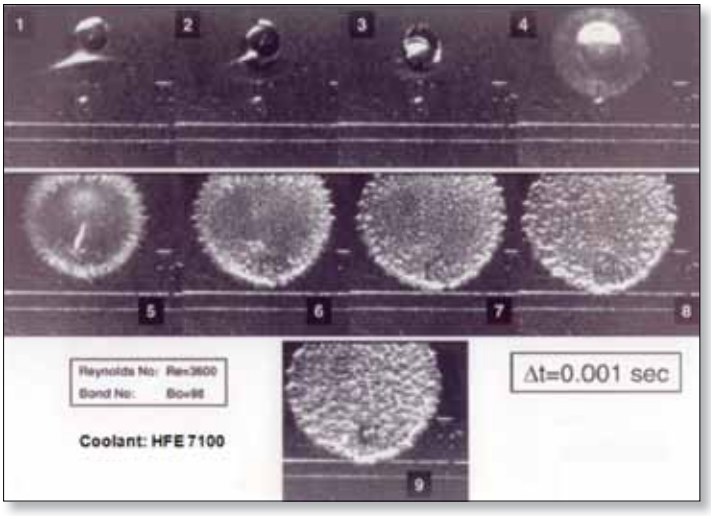

FIGURE 1: Test data- droplet impact.

INTRODUCTION

SPRAY COOLING processes yield high heat transfer coefficients due to heat absorption associated with latent heat absorption during liquid-vapor phase transition [1-5]. Spray cooling advantages lie in potentially eliminating TIM1 and TIM 2 thermal resistances, yielding significant reduction in overall thermal resistance.

Due to the complexity and chaotic nature of millions of high velocity spray droplets emanating from a nozzle interacting with a heated surface, droplet fragmentation/coalescence, fluid layer formation, imbedded vapor regions and vapor partial pressure effects affect evaporation rate and changes in temperature-dependent thermophysical properties (surface tension, viscosity, conductivity and specific heat, for example). These transient, micron scale droplet-wall interactions produce a statistical time series of locally varying heat transfer coefficients that, when averaged over area and time, yield an average heat transfer coefficient. Given different coolant types, spray injected at different droplet sizes and velocities onto walls of different roughness and spatial orientation, and considering the wide variety of thermophysical properties for different coolant types and wall materials that affect the spray cooling heat transfer coefficient, a large test matrix is required to determine the best combination of parameters to produce the highest av-

nozzle gauge pressure (kPa)	droplet dia. (microns)	avg. droplet dia. (microns)	delivery droplet velocity (m/s)	coolant flow rate (ml/sec)	maximum cooling potential (W/cm^2)
34.5	100 to 200	162	3.0 - 4.2	1.37	29.2
68.9	60 to 150	75	8 (max)	1.80	38.6
207	20 to 80	na	10 (max)	3.04	63.6

TABLE 1: Spray test data.

erage heat transfer coefficient. The many variables involved usually preclude an optimum selection of parameters to achieve this result. To limit use of test methods involving multiple sets of parameter combinations, recourse to CFD methods has advanced as an alternative to select the best combination of parameters producing the highest heat transfer coefficient for a given heat transfer case.

By use of a high speed (6000 frames/s) magnifying digital camera, observation of droplet impact dynamics and evaporation phenomena compared to CFD predictions provide qualitative verification that computer solutions reproduce test-observed micro-phenomena. From test measurements of evaporation times of different size droplets impacting a heated surface and comparison to CFD predictions, quantitative verification of the predictive capability of the commercial CFD software code [6] is confirmed in principle.

TEST RESULTS

Table 1 shows digital camera test results determining spray/droplet impact characteristics for an enclosure housing containing an array of nozzles. For a given nozzle, supply pressure determines the range of droplet diameters permitting an average droplet diameter to be used in CFD calculations. Atmospheric pressure is maintained in the test chamber. The corresponding average droplet velocity, flow rate and cooling potential based on complete evaporation of droplets are shown in Table 1. Test data shown are used as input parameters in CFD models.

Figure 1 shows the time progression of an HFE 7100 2 mm diameter (D) droplet at V = 72 cm/s vertically impacting a flat plate maintained above the droplet evaporation temperature of 334.5 K. The formation of vapor bubbles continues past 0.001s with total evaporation at ~0.35s. Droplet impact initiates at frame (4), followed by a vapor bubble outer fringe at (5) then interior droplet vapor bubble formation as the droplet flattens out in frames (6) to (9). Past 0.35s, evaporation is complete.

CFD transient results [7] are shown for a HFE 7100 20μm droplet on a heated surface that is maintained above evaporation temperature. These results verify the commercial CFD software code's [6] capability to provide a qualitative measure of the creation of vapor bubbles once internal droplet evaporation temperature and heat absorption latent heat conditions are attained.

For all test cases, data obtained for average droplet size and velocity are used as input for CFD runs to verify the CFD software code's capability to generate qualitative agreement with transient droplet impact phenomena and generation of vapor cavities. Since both CFD and test vapor cavities are chaotic in size, growth and location, only qualitative comparisons between test and computer results at a given time under similar conditions are possible. Nevertheless, the presence of similar qualitative features between test and CFD results is a necessary first step to show applicability of CFD methodology to represent features of real spray-surface interactions.

CFD METHODOLOGY AND RESULTS – EXPLORATION OF MICRO-DETAILS OF DROPLET-HEATED SURFACE INTERACTION

Figures 2 and 3 show a plane-cut, single time snapshot of a cold 335K, 80μm spherical water droplet at 515 cm/s impacting an initial fluid layer 10μm thick whose depth, temperature and free surface geometry have been affected by prior impacted droplets. Wall heat flux is maintained at 60 W/cm^2. A sequence of figures at different times during impact provide micro-details of droplet impact dynamics that determine fluid dynamic and heat transfer phenomena over larger areas impacted by numerous droplets. Figure 2 shows a cold water droplet merging with a warmed fluid layer created by prior droplet impacts- here, the wall fluid layer is being heated by conduction with the fluid zone away from the impact point reaching evaporation temperature-but not the latent heat enthalpy value (hfg) necessary for phase change. The arrival of cold droplets and subsequent mixing with the warmed fluid wall layer limits local impact zone fluid temperatures to reach evaporation temperature; thus, showing that heat transfer is generally limited by the formation of fluid surface layers maintained below evaporation temperature. Figure 3 shows details of the velocity distribution during the droplet-fluid wall layer merging process. Note the formation of a heated air void region at the droplet-fluid layer interaction zone caused by prior droplet impacts causing free surface waves to outwardly propagate in the coolant wall layer.

A corresponding figure for the internal wall temperature [7] at the same time as that for Figures 2 and 3 provides data to determine a localized heat transfer coefficient h. Time-sequenced, transient internal wall temperature data averaged over time and contact area as droplet impact and surface wall layer mixing progress then provides the means to determine the heat flux and an average h value. Reference [7] provides results for multiple droplet clouds impacting a localized wall area covered by a fluid surface layer. As impacting, closely

spaced droplets have complex, highly nonlinear interaction effects with the wall coolant layer, modeling multiple, closely separated droplets in three dimensions more closely resembles fluid and heat transfer phenomena associated with sprays emanating from a nozzle and can produce a refined estimate of the time and space-averaged heat transfer coefficient. Of practical interest is the use of spray cooling for very high heat flux conditions ~100-300 W/cm^2. Reference [7] presents high mass flow cases that constitute an approach to increased cooling through use of a large number of closely-spaced droplets impacting a hot surface undergoing evaporative heat transfer. Results indicate that higher droplet injection velocities together with larger droplet diameters impacting a wall coolant layer can result in impact craters leaving voids in the surface fluid layer. Such cases depend upon droplet size and spray velocity and limit evaporative cooling. Droplet fragmentation can also result from high speed droplet impact with the wall fluid layer which further reduces the heat transfer coefficient as fragmentary fluid bits are not in contact with the wall and not subject to evaporation. Thus, increased spray mass flow does not necessarily yield a higher average heat transfer coefficient.

CFD analysis [7] is used to provide additional insight into the effects of surface roughness, droplet speed, droplet diameter, different coolant types and high/low heat flux conditions for multiple droplet cloud cases insofar as these effects alter h values. For high heat flux cases, surface roughness patterns can provide a means of obtaining high h values beyond those possible for smooth wall surfaces.

HEAT TRANSFER COEFFICIENT CALCULATION PROCEDURES AND APPLICATION TO PRACTICAL PROBLEMS

The convection heat transfer coefficient, h, describing heat transfer between the heated surface and coolant droplets impinging on a heated surface with an associated coolant layer is defined below.

Definition of average heat transfer convection coefficient

$$h \approx \frac{1}{A_f} \frac{\delta Q}{\delta t \cdot \delta T}$$

where,

h is average convection coefficient

A_f is effective surface sub-area impinged by spray coolant droplets

Q is heat transferred into the coolant

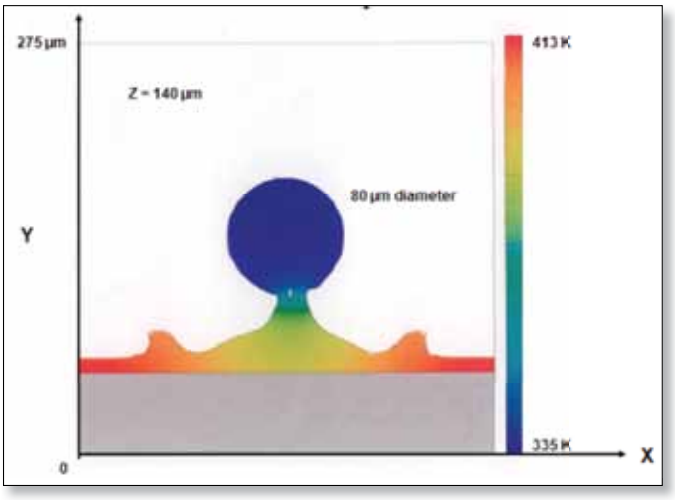

FIGURE 2: CFD coolant temperature.

δt is difference in time used for the CFD calculation domain

δT is temperature difference between the average temperature of the heated surface and the saturation temperature of the spray coolant

To determine h for a particular application, first spray characteristics are determined from high speed camera tests (typical of Table 1) or from nozzle manufacturer spray specifications given a supply pressure value corresponding to a given coolant flow rate. These data provide average droplet size and average droplet velocity. Given the nozzle flow rate at a given supply pressure and assuming a uniform spray distribution over the total heat transfer area (A), the number of droplets (n) of given mass (m) and diameter (D) impinging on a sub-area (A_f) of A over a given time (δt) can be determined to match area-scaled mass flow considerations. This permits an estimation of (or test-observed) average lateral and vertical droplet spacing. A CFD model of n properly spaced droplets in three-dimensions forming a droplet cloud is modeled with a given velocity that will impact A_f. CFD calculations are next run to determine the heat removed from the wall over δt given a prescribed heat flux magnitude within the die. This step involves the dimensional geometry of the die volume (V), wall thermophysical properties and the wall roughness pattern (if present) and the wall orientation with respect to the spray pattern. From the time and space averaged, steady-state CFD solution, the through-wall temperature difference and heat transfer (δQ) extracted from V is available and the $h = \delta Q / A_f \delta t \, \delta T$ definition is applied where $\delta T = T_{surf} - T_{sat}$ and where T_{surf} is the average wall surface temperature over Af from multiple droplet cloud impacts in time δt. Presuming that the local *h* value over A_f extends over all of A as the flow distribution from the nozzle is spatially uniform, then an average *h* is determined for a specific die geometry and die wall roughness pattern for a specific heat transfer application.

SELECTION OF CONDITIONS FOR OPTIMAL HEAT TRANSFER COEFFICIENT

Figure 4 shows the commercial CFD software code's calculated results for heat loss Q from a given heat transfer volume with an internal heat flux of 30 W/cm^2 with surface area A for 20µm HFE 7100 spray droplets. The curves shown are for cumulative droplet flow rates ranging from a low 0.02 to high 2.0 cm3/s per cm^2 of surface area and represent the transient heat loss development over time from initiation of spray cooling on the surface of a die material volume initially at room temperature. Of interest is the long-time extent of these curves as steady state operation is approached.

Larger h values constant with time are expected for intermediate flow rates as indicated in Figure 4; at extreme low and high flow rates, h values can fluctuate in time and location due to phenomena described by [7]. While intermediate flow rates apparently lead to optimal h values, smaller droplet sizes are advantageous (~ 20-50µm) as their smaller mass leads to more rapid heating, less tendency to cause splattering and splashing, and short evaporation times.

From Figure 4, curves that peak then decrease for higher flow rate cases indicate that heat loss ultimately decreases with increasing time by the effects previously described once initial heat-up transients pass. For lower flow rates, heat loss decreases due to fluid burnout/loss on the (flat) heated surface and the absence of evaporative cooling replaced by free convective cooling at much lower heat transfer rates. Figure 4 indicates that higher flow rates always produce higher heat loss than lower rates but optimizing heat transfer lies mainly in selection of coolant thermophysical properties, droplet diameter and velocity. The predicted maximum h value shown in Figure 5 is 1 to 2 W/cm^2 °C, which is comparable to measured values indicated by Isothermal Systems Research (ISR) through communications in 1998 for the multi-nozzle spray head enclosure referenced in Section 1, Test Results. Results shown are

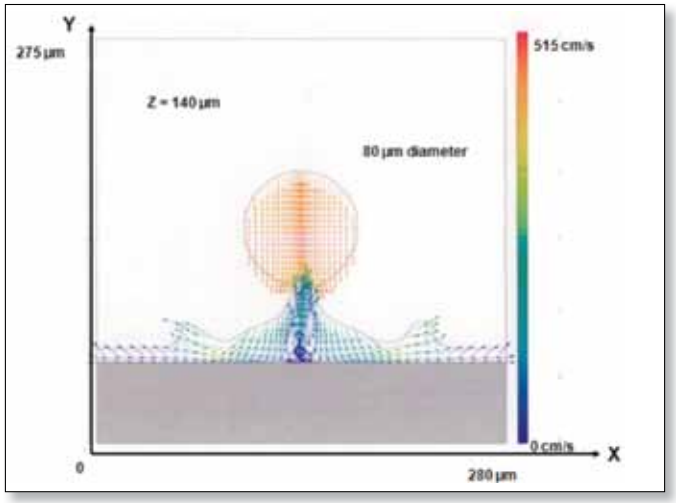

FIGURE 3: Internal droplet and wall layer Velocity distribution.

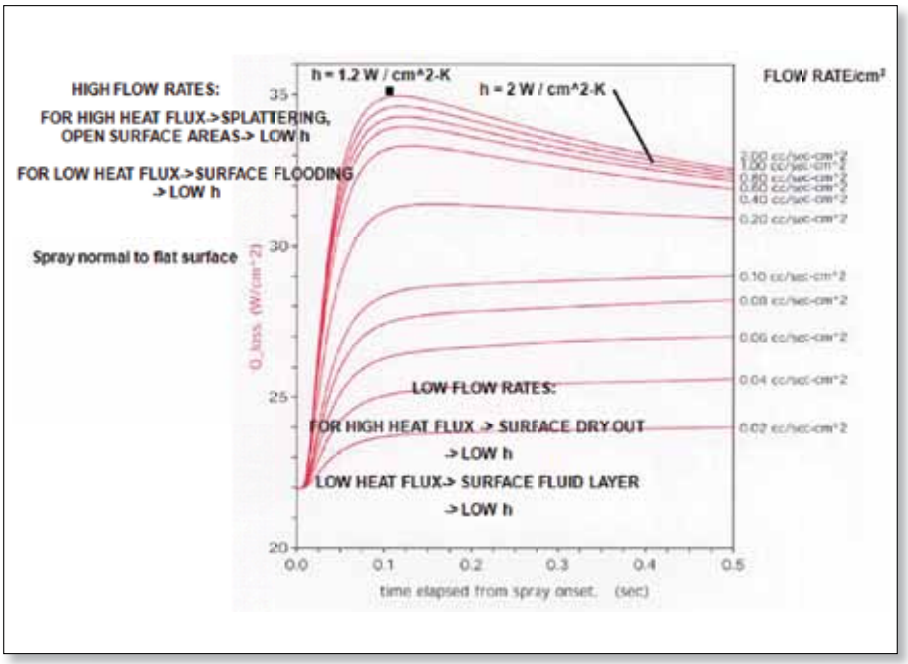

FIGURE 4: Heat loss with time.

for smooth wall surfaces but different microscale surface roughness patterns show promise to increase h values [7].

Figure 5 shows plots of $T_{surf} - T_{sat}$.

For low flow rates (mass of droplets passing through an area A in time δt), wall temperature continually increases while for high flow rates, lower wall temperatures result. Since splattering and coolant layer open void areas can occur at higher spray flow rates as shown in [7], wall temperature increases as the effective evaporative heat removal mechanism is reduced. The fluid dynamic/heat transfer effects at low and high flow rates for low and high heat flux conditions previously described apply so that an intermediate flow rate that prevents unsteady heat transfer conditions from occurring is the best option for sustained high h values. The use of grooved, microscale wall surface roughness

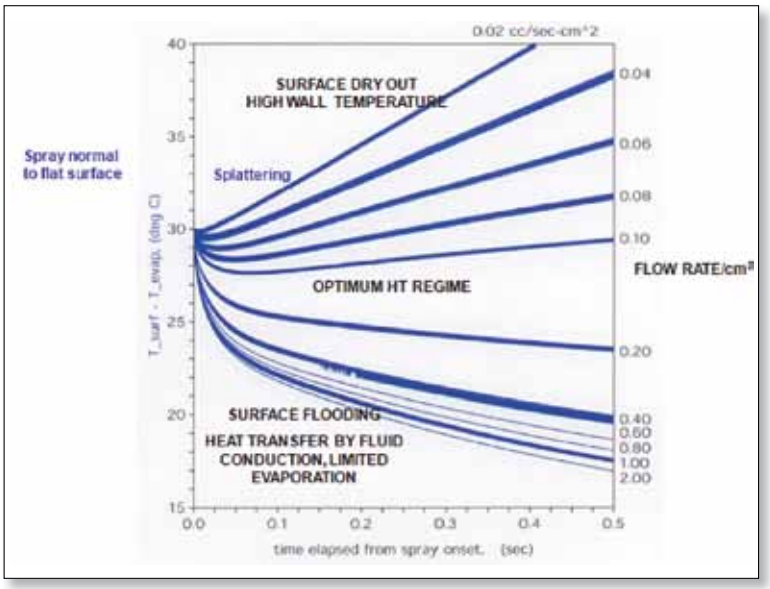

FIGURE 5: Temperature change vs. time.

to increase heat transfer coefficient has the potential to increase h values as indicated by Reference [7] results; however, such extensions to increase h values remain to be fully explored in future research.

Results from Figures 4 and 5 are specific to parameters selected (heat flux, coolant type, droplet size, droplet velocity and spatial distribution, flow rate, etc.). Further discussion of other parameter variations is provided in Reference [7].

CONCLUSIONS

An estimate for heat transfer coefficients, used to develop Figures 4 and 5, is available through a developed program that incorporates parameter variation studies to aid in estimation of average h values. For specific applications, further verification tests must follow after use of CFD results that provide foundation data, to isolate key parameters that have the most influence on obtaining optimal heat transfer coefficients. Correlation equation development only through tests entails a large test matrix involving many variations of key parameters; this procedure is usually economically impractical and time-consuming. By using selected test results for spray characteristics together with recourse to CFD examples that provide data for different size (and material type) coolant droplet clouds at different velocities, this alternative then provides micro-details of droplet-heated wall and droplet-fluid wall layer interaction to serve as a guide to understand the complex fluid dynamic and heat transfer process underlying predicted heat transfer coefficient values. Since high heat flux values are of interest for the next generation of electronic cooling applications, generalizations drawn from results shown in Figures 5 and 6 can prove useful to evaluate effects of different parameter variations on heat transfer and provide guidance for best parameter choices in verification tests to follow.

In summary, for high spray flow rate, high heat flux cases, droplet splattering can occur inducing open wall fluid layer void areas leading to low h values. For low heat flux conditions, surface flooding can occur limiting evaporative cooling resulting in low h values. For low flow rate, high heat flux conditions, wall dry spots result again producing low h values. For low heat flux and low flow rates, surface flooding and thick wall layers develop limiting evaporative cooling. Results are for flat, horizontal heat transfer surfaces with normal spray patterns; surface inclination to limit wall fluid layer buildup should increase the effectiveness of spray cooling substantially. The predicted h values shown in the example cases would have the potential to yield acceptable cooling capability for the majority of the high powered ASIC used for blade server and TELCO router applications. For example, a 77°C maximum, "hot spot" junction temperature would be attained for a lidless ASIC having a 3 cm^2 silicon foot print that is dissipating a total power of 128W while having a maximum hot spot power density is equal to 2 times the overall average power density of 42.7 W/cm^2 within the silicon if h = 2 W/cm^2 °C, and a 30°C spray coolant droplet temperature impinges on the inactive side of the silicon. The example cases presented in this brief summary (as well as other examples) are further detailed in [7]. The methodology and computer methods shown point to a new understanding of spray cooling micro-phenomena and its practical use for electronic cooling applications, and show promise to guide test experimentation to determine optimal heat transfer coefficients for high heat flux applications.

REFERENCES

[1] B. Horacek, K. Kiger and J. Kim (2005) Single Nozzle Spray Cooling Heat Transfer Mechanisms International, Journal of Heat and Mass Transfer, Vol.8, Issue 8.

[2] Z. Yan, K. Toh, F. Yuan, T. Wong, K. Chao, K. Chan and P. Chua (2010) Heat Transfer Characteristics of Impingement Spray Cooling Systems for Electronic Test Cards. Proceedings of Computer and Automation Engineering 2nd International Conference, Singapore.

[3] J. Kim (2007) Spray Cooling Heat Transfer: The State of the Art International Journal of Heat and Fluid Flow, Vol. 28, Issue 4.

[4] W. Cheng, Q. Liu, R, Zhao and H. Fan (2010) Experimental Investigation of Parameter Effects on Heat Transfer of Spray Cooling. Journal of Heat and Mass Transfer, Vol. 46, No. 8-9.

[5] B. Horacek, J. Kim and K. Kiger, (2004) Spray Cooling of Singular and Multiple Nozzles: Visualization and Wall Heat Transfer Measurements. IEEE Transactions on Device and Materials Reliability, Vol. 4, Issue 4.

[6] Trademark name: FLOW-3D.

[7] C. Ortloff, M. Vogel, (2011) Spray Cooling Heat Transfer – Test and Analysis Results. Proceedings of the 27th Annual IEEE Semiconductor Thermal Measurement and Management Symposium.

Lidded Versus Bare Die

Flip Chip Package: Impact on Thermal Performance

Jesse Galloway, Amkor Technology Inc.

Jesse Galloway is a Vice President at Amkor Technology supporting thermal development of electronic packages. He has over 20 years experience in electronic cooling. He received his Ph.D. in Mechanical Engineering from Purdue University. His areas of expertise include experimental testing, numerical simulation and simulation automation. Jesse has published over 30 publications.

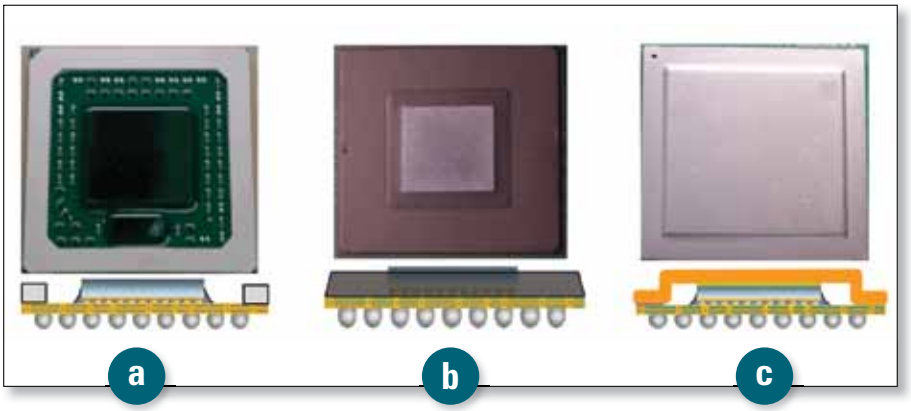

FIGURE 1: Styles of FCBGA packages. (a) Stiffener window FCBGA, (b) FCmBGA, (c) FCLBGA.

Heat Sink	Material	Theta sa (C/W)	Length (mm)	Width (mm)	Height (mm)	Base Thickness (mm)
A	Copper	0.52	79	89	52	7.7
B	Aluminum	1.56	70	70	14	3.90
C	Aluminum	2.54	44	31	16	2.9

TABLE 1: Heat sink description.

INTRODUCTION

THERMAL DESIGN and material selection continues to be a concern for electronic packages; particularly for flip chip ball grid array packages (FCBGA). Lower cost package options are available today, which are finding applications in high power design spaces that previously only employed copper lid heat spreaders. Exposed die flip chip packages are used frequently in lower power applications where the die size is relatively small (less than 8mm). Larger die sizes exhibit greater package warpage due to the difference in thermal expansion coefficients between silicon and laminate materials. As a result, large die packages are more difficult to solder mount and may produce larger variations in the bond line thickness between the die and external heat sinks. Two options are available to reduce the package warpage. The first option, shown in Figure 1(a), is to mount a stiffener window to the periphery of the package in order to provide structural rigidity. A second and lower cost option is to underfill the die and mold the body of the package in a single process step. This style of package, as shown in Figure 1(b), is called a flip chip molded ball grid array (FCmBGA). The most common style of package is the flip chip lidded ball grid array (FCLBGA), as shown in Figure 1(c). A copper lid is mounted to the die back-side with thermal interface material (TIM I) between the lid and die. An added benefit of the exposed

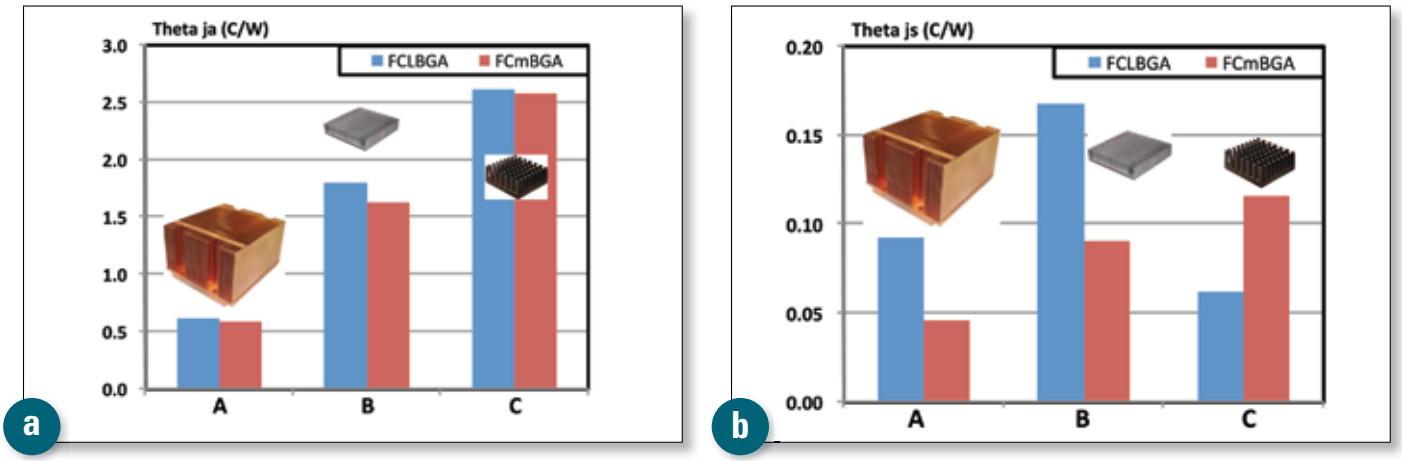

FIGURE 2: Theta js and Theta ja resistance as a function of FCLBGA and FCmBGA packages for three different heat sinks.

die package options, Figure 1(a) and 1(b), is the elimination of the thermal interface material (TIM I). For exposed die packages, only one interface is needed (TIM II) between the die and heat sink.

EXPERIMENTAL MEASUREMENTS

This study reports measurements made with FCmBGA and FCLBGA packages as a function of heat sink size. Both styles of packages have a 45mm body size with an 18mm die. Experimental measurements were made using packages shown in Figure 1(b) and 1(c) with three different size heat sinks as described in Table 1. A relatively low thermal resistance TIM II, 15C- mm^2/W, was used to gather the data reported here. A more detailed description may be found in Galloway and Kanuparthi [1]. Theta js is defined as the maximum junction temperature (measured at center of die), less the heat sink temperature (measured at a location centered on the heat sink base), divided by the supplied power. Theta js is useful in characterizing the performance of the package and TIM II. The FCmBGA style package has a lower thermal resistance when the heat sink base can adequately spread the heat, see Figure 2(a). A thicker heat sink base with a higher conductivity material promotes greater spreading of heat away from the die. Heat sink C has a relatively thin base and is made from a lower conductivity material (aluminum). As a result the lidded package, even though it has an additional TIM layer, produces a lower Theta js due to the design of heat sink C. Theta ja provides a measurement of the total resistance including the combined resistance of the heat sink, TIM II and package, see Figure 2(b). A slight reduction in Theta ja was measured for heat sinks A and B with the FCmBGA package. Theta js is approximately 25X lower than Theta ja for heat sink C. Hence no appreciable differences in Theta ja was measured for heat sink C even though Theta js was lower for the FCLBGA package.

NUMERICAL SIMULATIONS

To provide a more detailed understanding of the impact of TIM II material on Theta ja, a finite element analysis (FEA) study was conducted to predict Theta ja as a function of package style (FCLBGA versus FCmBGA) and TIM II resistance for 6mm, 10mm and 18mm die. As one may expect, for low TIM II resistance, the FCmBGA package provides the low-

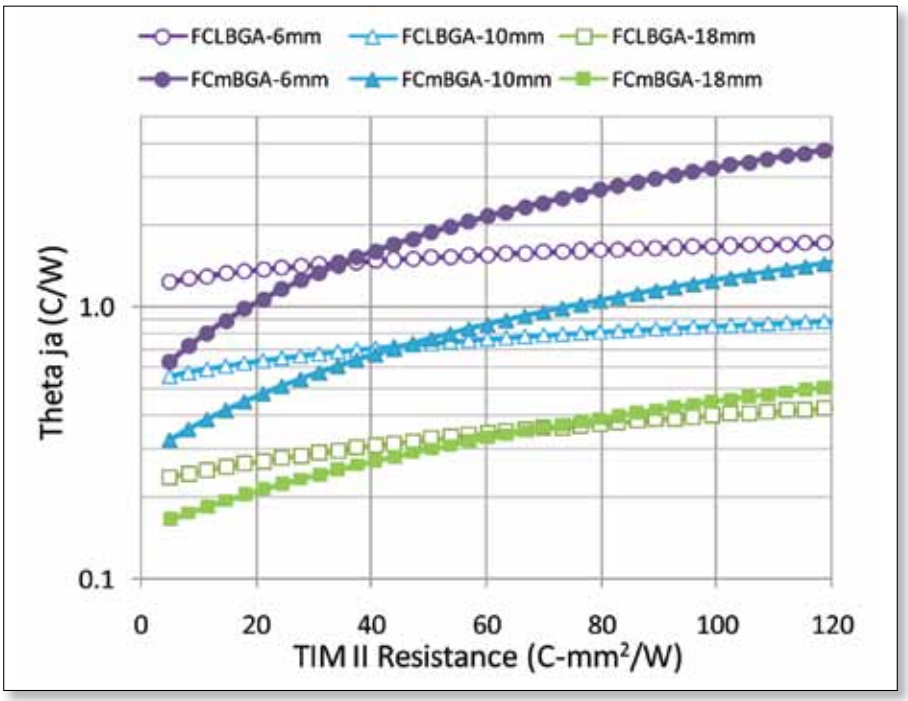

FIGURE 3: Theta ja vs. TIM II resistance for 6mm, 10mm, 18mm die.

est thermal resistance since there is only one interface (TIM II) whereas the FCLBGA has two interfaces, TIM I and TIM II.

The TIM II interface can become a dominant factor if the bond line thickness (BLT) is large. In certain cases, system level designs cannot control the BLT at the TIM II layer due to component stack-up variations, e.g. when the de facto heat sink is an EMI shield or a system chassis. For these cases, a gap filler TIM II must be used. Gap filler TIMs, as their name suggests, are relatively thick/low modulus materials that conform to the gap available between the package top surface and the heat sink. FCmBGA Theta ja variation with TIM II resistance has a steeper slope compared to the FCLBGA package. Adding a lid tends to spread the heat over an area larger than the die, thus reducing the TIM II resistance. However, for larger die sizes, the difference between FCLBGA and FCmBGA Theta ja becomes smaller. The Theta ja resistance cross-over point, where the FCLBGA resistance is equal to the FCmBGA package, occurs at a TIM II resistance of approximately 45°C- mm²/W.

CONCLUSION

The FCmBGA package style offers an attractive means for reducing the overall package resistance. To achieve these benefits, a lower resistance TIM II material will be required.

REFERENCES

[1] Galloway J. and S. Kanuparthi, "Thermal performance of FCmBGA: Exposed molded die compared to lidded package" Semiconductor Thermal Measurement and Management Symposium (SEMI-THERM), 2011, 27th Annual IEEE, March 2011, pp. 181 - 186.

Index of Advertisers

Alpha's Next Generation Heat Sink

Custom or off-the-shelf.
Simple to complex.
Prototype to mass production.

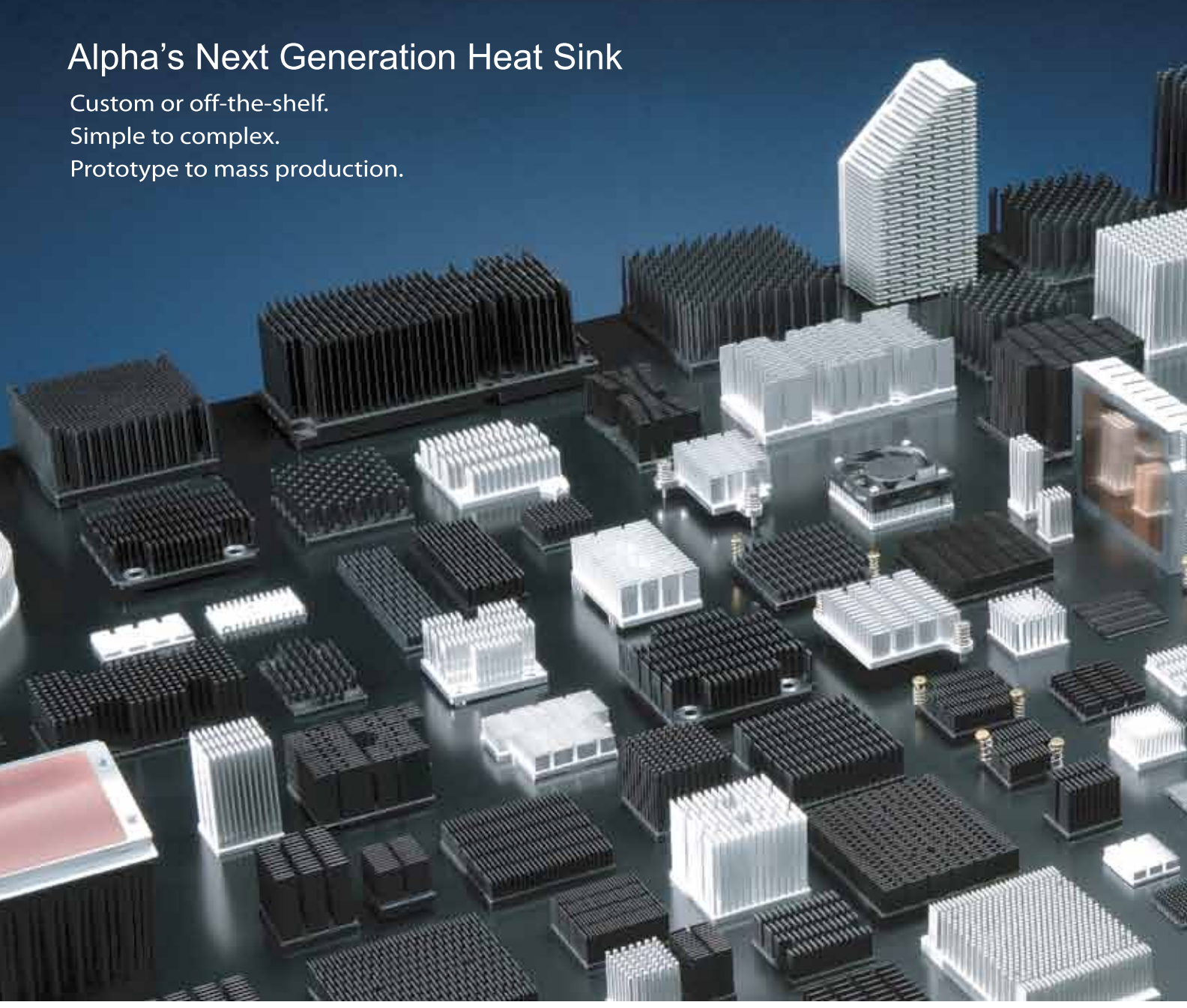

QSZ Clip

Minimum PCB Area

Pins only require 1.8mm diameter holes in the PCB.

Mounting Security

Easy-Install

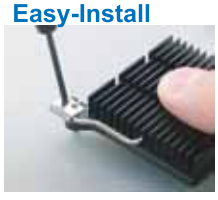

ALPHA SUPPORT

Variety of catalog parts : The most suitable heat sink, for many different environments, can typically be found from Alpha's standard catalog.

Data Library : Download CAD files, Flotherm data models and RoHS CofC from Alpha's website.

Engineering Support : Alpha provides thermal solutions with a focus on short lead times and low cost while providing outstanding customer support.

ALPHA

Your partner for thermal solutions

ALPHA Co., Ltd.
Head Office
www.micforg.co.jp
256-1 Ueda, Numazu City, Japan 410-0316
Tel: +81-55-966-0789 Fax: +81-55-966-9192
Email: alpha@micforg.co.jp

ALPHA NOVATECH, INC.
USA Subsidiary
www.alphanovatech.com
473 Sapena Ct. #12, Santa Clara, CA 95054 USA
Tel:+1-408-567-8082 Fax: +1-408-567-8053
Email: sales@alphanovatech.com

s-force...

the highest performing fans on the market

Whether for cooling server rooms or switch cabinets, complex machines or sensitive medical technology - our intelligent and controllable high performance fans can be suited for many different applications!

- Optimum motor efficiency and long service life.
- Reaches nominal speeds up to 14,000 rpm and operating values previously attained by larger fans or blowers.
- Increase in overall fan efficiency and lowered acoustics at relative operating points.
- Five series with sizes ranging from 3.2 in (80 mm) to 8.77 in (220mm).

www.ebmpapst.us

GREEN TECH

ebmpapst